

**CARBON FIBER COMPOSITES PREPARED FROM  
ORGANOCLAY-AEROSPACE EPOXY NANOCOMPOSITES**

**Thesis**

**Submitted to**

**Graduate Engineering & Research  
School of Engineering of the**

**UNIVERSITY OF DAYTON**

**In Partial Fulfillment of the Requirements for**

**The Degree**

**Master of Science in Chemical Engineering**

**by**

**Larry Allan Cloos**

**UNIVERSITY OF DAYTON**

**Dayton, Ohio**

**May 2001**

**CARBON FIBER COMPOSITES PREPARED FROM ORGANOCLAY-  
AEROSPACE EPOXY NANOCOMPOSITES**

**APPROVED BY:**

---

**Kevin J. Myers, D.Sc, P.E.**  
Advisory Committee Chairman  
Professor, Department of Chemical  
and Materials Engineering

---

**Chenggang Chen, Ph.D.**  
Research Advisor  
Nonmetallic Division  
University of Dayton Research Institute

---

**William Lee, Ph.D.**  
Committee Member  
Professor, Department of Chemical  
and Materials Engineering

---

**Donald L. Moon, Ph.D**  
Associate Dean  
Graduate Engineering Programs &  
Research, School of Engineering

---

**Blake Cherrington, Ph.D., P.E.**  
Dean, School of Engineering

## ABSTRACT

### **CARBON FIBER COMPOSITES PREPARED FROM ORGANOCLAY-AEROSPACE EPOXY NANOCOMPOSITES**

Name: Cloos, Larry Allan  
University of Dayton, May 2001

Research Advisor: Dr. Chenggang Chen

Academic Advisor: Dr. Kevin J. Myers

A nanocomposite prepared from the addition of an organically-modified layer silicate to an epoxy was investigated as a matrix resin for carbon fiber composites. The nanocomposite consisted of a I.30E, a montmorillonite clay treated with *n*-octadecylamine and HCl and Epon Resin 862 / Epicure Curing Agent W, an aerospace epoxy resin. This resin was used along with IM7G-12k tow carbon fiber to process continuous unidirectional carbon fiber composites via two methods, resin film infusion and wet-winding. The characterization included possible barrier enhancements such as decreased solvent uptake and thermal oxidative stability. Matrix dominated mechanical properties were investigated using a transverse four point flex test and an axial four point shear test. A thermal analysis was performed to determine the effect of layer silicate addition

on coefficients of thermal expansion and glass transition temperatures.

Composite quality was investigated using acid digestion, scanning electron microscopy, and photomicroscopy.



## ACKNOWLEDGEMENTS

First, I would like to extend my sincere gratitude to my research advisor, Dr. Chenggang Chen, and Brian Rice. Each of you offered me your time and knowledge. Your experience and advice has genuinely aided me throughout my research project. I would also like to acknowledge Dr. David Curliss for providing the financial support for my research work under the aerospace composite materials contract F33615-00-D-5006. I want to thank Dr. Dave Anderson for always taking the time to answer my technical questions that inevitably arose. I would also like to acknowledge the University of Dayton Chemical Engineering Department. I have had the joy of having most of you as professors and am grateful for all that you have taught me. I have truly grown over these last two years and owe it to hard work and your devotion to teaching excellence. And last but not least, I would like to thank Mindi, my wife. Your support and patience throughout my masters degree and this research is appreciated and I love you.

## TABLE OF CONTENTS

ABSTRACT .....	iii
ACKNOWLEDGEMENTS .....	v
LIST OF FIGURES .....	viii
LIST OF TABLES.....	x
LIST OF SYMBOLS .....	xi
CHAPTER	
I. INTRODUCTION .....	1
II. REVIEW OF RELATED RESEARCH AND LITERATURE .....	3
2.1 EPON RESIN 862 / EPICURE CURING AGENT W.....	3
2.2 LAYERED SILICATES.....	6
2.3 INCORPORATION OF LAYERED SILICATES INTO A POLYMER .....	7
2.4 PREPARATION OF NANOCOMPOSITES.....	9
2.5 PROPERTIES.....	11
2.6 CARBON FIBER COMPOSITES .....	12
III. EXPERIMENTAL.....	13
3.1 SOLVENT UPTAKE – BARRIER PROPERTIES.....	13
3.2 THERMAL OXIDATIVE STABILITY TEST.....	13
3.3 CONTINUOUS UNIDIRECTIONAL CARBON FIBER	

COMPOSITE PROCESSING .....	14
3.4 ACID DIGESTION .....	15
3.5 SCANNING ELECTRON MICROSCOPY .....	19
3.6 PHOTOMICROSCOPY .....	20
3.7 MECHANICAL TESTING.....	20
3.8 THERMAL MECHANICAL ANALYSIS.....	21
IV. RESULTS AND DISCUSSION .....	22
4.1 SOLVENT UPTAKE – BARRIER PROPERTIES.....	22
4.2 THERMAL OXIDATIVE STABILITY TEST.....	24
4.3 ACID DIGESTION .....	25
4.4 SCANNING ELECTRON MICROSCOPY .....	30
4.5 PHOTOMICROSCOPY .....	33
4.6 MECHANICAL TESTING.....	34
4.7 THERMAL MECHANICAL ANALYSIS.....	39
V. CONCLUSIONS .....	41
REFERENCES .....	43

## LIST OF FIGURES

2.1	Chemical structure of Shell Epon Resin 862 .....	4
2.2	Chemical structure of Epicure Curing Agent W .....	5
2.3	Generalized epoxy-amine polymerization reaction.....	5
2.4	Organically-modified layered silicate .....	8
3.1	Layup procedure for RFI of epoxy-carbon fiber composite (autoclave)....	16
3.2	Layup procedure for RFI of epoxy-carbon fiber composite .....	16
3.3	Fiber composite wet-winding apparatus.....	17
3.4	Fiber composite wet-winding apparatus (resin bath/heat lamp shown)....	17
3.5	Fiber composite wet-winding apparatus (winding table).....	18
3.6	Fiber composite wet-winding apparatus (fiber plate shown) .....	18
3.7	Fiber composite wet-winding apparatus(resin bath/glass die shown) .....	19
4.1	Percent mass gain versus square root of time due to diffusion of water into Epon Resin 862 / Epicure Curing Agent W loaded with I.30E .....	26
4.2	Percent mass gain versus square root of time due to diffusion of acetone into Epon Resin 862 / Epicure Curing Agent W loaded with I.30E .....	27
4.3	Percent mass gain versus square root of time due to diffusion of methanol into Epon Resin 862 / Epicure Curing Agent W loaded with I.30E .....	28
4.4	TGA results of I.30E at ten degrees Celsius per minute in a nitrogen atmosphere .....	29
4.5	SEM micrograph of shear failure surface of Epon 862 / W / IM7 processed via resin fusion infiltration.....	30

4.6	SEM micrograph of shear failure surface of Epon 862 / W / 6% I.30E / IM7 processed via resin fusion infiltration.....	31
4.7	SEM micrograph of shear failure surface of Epon 862 / W / IM7 processed via wet-winding.....	31
4.8	SEM micrograph of shear failure surface of Epon 862 / W / 3% I.30E / IM7 processed via wet-winding .....	32
4.9	SEM micrograph of shear failure surface of Epon 862 / W / 6% I.30E / IM7 processed via wet-winding .....	32
4.10	SEM micrograph of shear failure surface of Epon 862 / W / 9% I.30E / IM7 processed via wet-winding .....	33
4.11	Photomicrograph of Epon 862 / W / IM7 processed via wet-winding .....	35
4.12	Photomicrograph of Epon 862 / W / 3% I.30E / IM7 processed via wet-winding .....	35
4.13	Photomicrograph of Epon 862 / W / 6% I.30E / IM7 processed via wet-winding .....	36
4.14	Photomicrograph of Epon 862 / W / 9% I.30E / IM7 processed via wet-winding .....	36
4.15	Photomicrograph of Epon 862 / W / IM7 processed via RFI .....	37
4.16	Photomicrograph of Epon 862 / W / 6% I.30E / IM7 processed via RFI ...	37

## LIST OF TABLES

4.1	One-dimensional binary diffusion coefficients of various solvents in Epon Resin 862 / Epicure Curing Agent W .....	23
4.2	Effects of silicate addition on thermal oxidative stability .....	25
4.3	Fiber volume fractions of Epon Resin 862/Epicure Curing Agent W/IM-7 composites.....	25
4.4	Mechanical properties of Epon 862 / W / I.30E / IM7 composites .....	39
4.5	Thermal-mechanical analysis of fiber composites and resin plaques.....	40

## LIST OF SYMBOLS

$b$	Width
$h$	Half-thickness
$D$	One-dimensional binary diffusion coefficient
$L$	Span
$M_{\max}$	Maximum percent mass gain
$P$	Load
$t$	Thickness
$T$	Temperature
$\Delta E$	Change in Enthalpy
$\Delta F$	Change in Helmholtz Free Energy
$\Delta M/\Delta t^{1/2}$	Initial slope of the percent mass gain verse square root time plot
$\Delta P/\Delta v$	Initial slope of stress verse strain curve
$\Delta S$	Change in Entropy
$\pi$	$\pi = 3.14159.....$

## CHAPTER I

### INTRODUCTION

Industry incorporates fillers into polymers as a means of imparting improved properties to the polymer such as increased tensile properties, reduced solvent uptake, and flame retardancy. It is also a good way to reduce the overall product cost, as the filler is generally a fraction of the cost of the polymer material. Recently, a new class of nano-sized particles has emerged as a promising replacement for conventional fillers.

Nanocomposites are a hybrid material, which combine a polymer matrix with a nano-sized reinforcement phase. The reinforcement will have one, two, or three dimensions approximately nanometer-sized. These materials have created improved properties over previously used fillers such as calcium carbonate, glass fibers, and carbon black, and at much reduced loadings [8]. The main obstacle associated with their use in composite matrices is the inherent incompatibility of the inorganic reinforcement with organic polymer matrix materials.

One nano-sized reinforcement has been studied intensely; montmorillonite clay. It is typically 1 nanometer thick with x and y dimensions ranging from 20 nanometers to 200 nanometers. It is a 2:1 layered silicate with a high specific area ( $760\text{m}^2/\text{g}$ ) [11] and possesses an intermediate charge density, making it a



good candidate for ion exchange reactions. By replacing the inorganic cations that reside along the surface of the layered silicate with organic surfactants, the clay is compatibilized with the organic matrix. Proper selection of the surfactant is vital to achieving complete dispersion of the clay platelets within the polymer. Without complete dispersion, or exfoliation, maximum property improvements will not occur.

The use of layered silicates offers new hope for improvements in carbon fiber composite technology. As the in-plane properties of a carbon fiber composite are dominated by the fiber, the z-axis properties are limited by the composite matrix. The incorporation of layered silicates into carbon fiber composite matrix material may lead to enhancements, which could open the door to new uses and use in more aggressive environments.

## CHAPTER 2

### REVIEW OF RELATED RESEARCH AND LITERATURE

#### 2.1 EPON RESIN 862 / EPICURE CURING AGENT W

The polymer system studied in this research consists of Epon Resin 862 and Epicure Curing Agent W. The Epon Resin 862 is a thermoset epoxy resin supplied by Shell. It is a low viscosity (25-45 Poise at 25 °C), liquid epoxy resin manufactured from epichlorohydrin and Bisphenol-F. It has an epoxide equivalent weight of 166-177 and a density of 9.9 lb/gal [18]. Its chemical structure is shown in Figure 2.1. Notable characteristics of Epon Resin 862 include low viscosity, excellent resistance to chemicals, and superior physical properties compared to diluted high viscosity resins. It also reacts with a wide range of standard epoxy curing agents. The major benefits are reduced diluent, increased flow in cold environments, and improved fiber and filler wetting. Thus, it is a suitable choice for a carbon fiber composite matrix. Crystallization is possible at temperatures between the glass transition temperature (-10 °C to -20 °C) and the crystalline melting point (80 °C to 85 °C) [18].

The curing agent used in this research is Epicure Curing Agent W, diethyltoluenediamine. Its chemical structure is shown in Figure 2.2. It is mixed

with Epon Resin 862 at a ratio of 100 parts Epon Resin 862 to 26 parts Epicure Curing Agent W.

The Epon Resin 862 / Epicure Curing Agent W system was chosen based on several factors. First, due to its low viscosity and low reactivity, it is suitable for carbon fiber composites processing techniques such as resin transfer molding (RTM) and vacuum assisted resin transfer molding (VARTM). Also, it has a high glass transition temperature ( $\sim 155\text{ }^{\circ}\text{C}$ ), which allows it to be used in higher temperature environments. The general amine-epoxy polymerization reaction is shown in Figure 2.3.

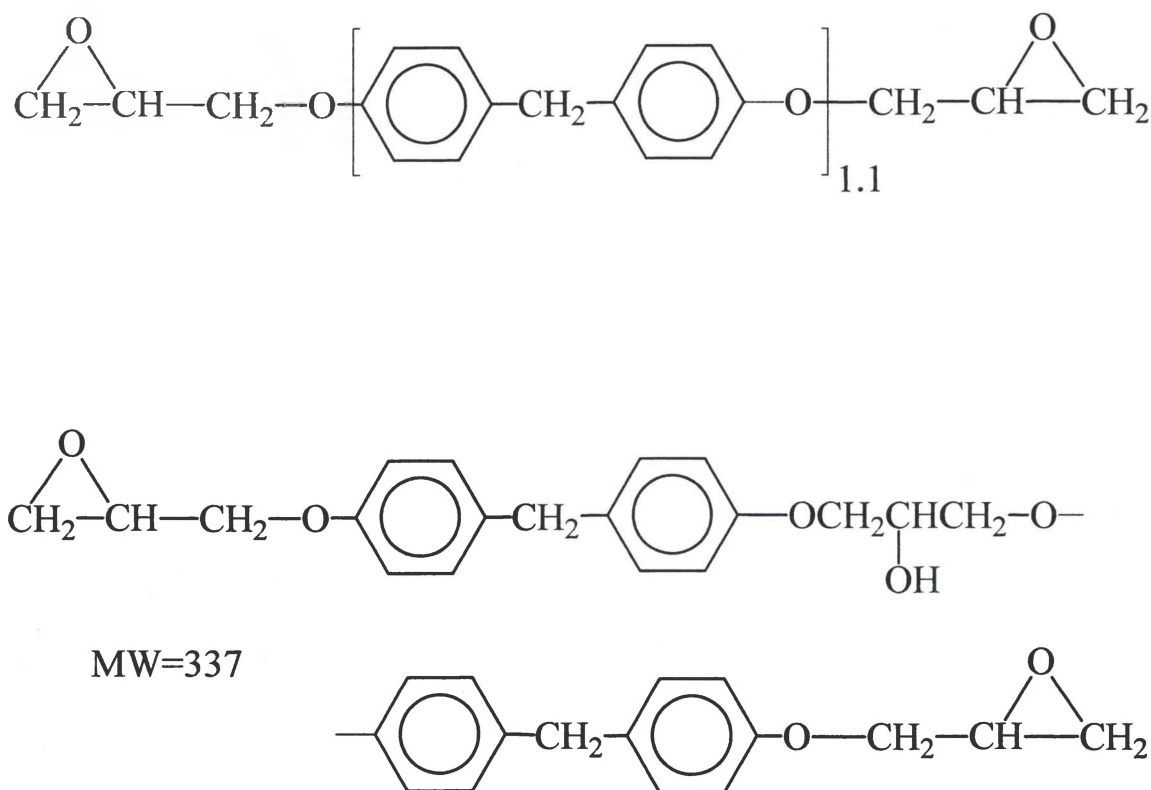


Figure 2.1. Chemical structure of Shell Epon Resin 862

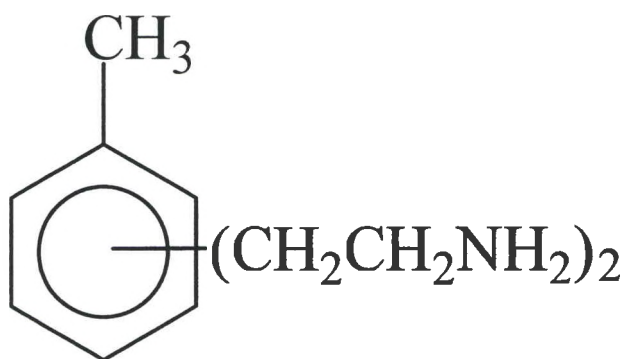


Figure 2.2. Chemical structure of Epicure Curing Agent W

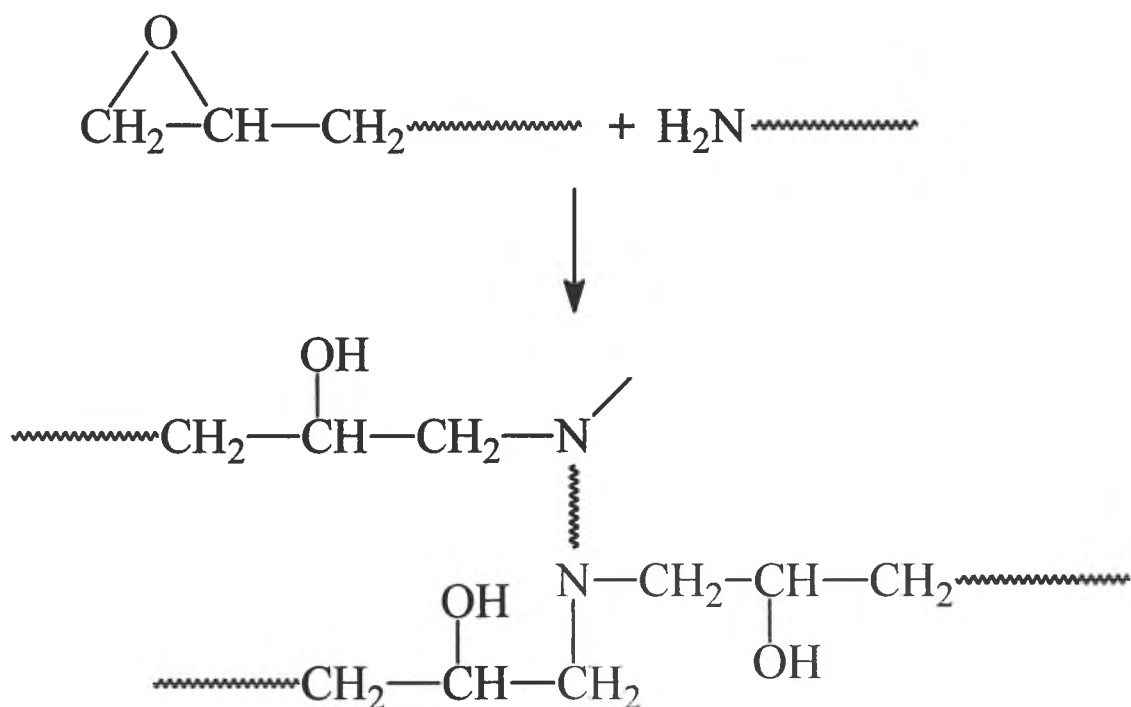


Figure 2.3. Generalized epoxy-amine polymerization reaction

## 2.2 LAYERED SILICATES

The most common clay used for polymer nanocomposites is montmorillonite. The structure is a 2:1 layered silicate with two inverted tetrahedral silicate layers sharing their apical oxygens with an octahedral aluminum layer. In montmorillonite, the layer charge originates from the substitution of octahedral  $\text{Al}^{3+}$  by  $\text{Mg}^{2+}$  [1]. The resultant surface charge in montmorillonite is intermediate and varies from 0.4 to 1.2e<sup>-</sup> per  $\text{Si}_8\text{O}_{20}$  unit [4]. To balance this negative layer charge, layers of hydrated cations are intercalated between the clay layers [4]. The structure of the clay is a face to face stack morphology, alternating between negatively charged silicate layers and positively charged gallery regions. It is possible for the gallery region to swell. The layer charge as well as the type of cations in the galleries of a clay determine the degree of swelling [4]. If the layer charge is high, the swelling is hindered due to the greater electrostatic attraction between the silicate surface and the gallery cations. When the layer charge is low, it is energetically easier to separate the layers from the gallery cations by adsorption of a polar solvent such as water [4]. The energy of solvation of the gallery cations as well as the interaction with the hydrophilic clay layer surfaces contribute to driving forces for intragallery adsorption [4].

The organoclay used for this research is I.30E. It is supplied by Nanocor, Arlington Heights, Illinois. It was made by the treatment of montmorillonite with *n*-octadecylamine and HCl. The pendent octadecylamine group makes the montmorillonite hydrophobic, thus compatibilizing it with the hydrophobic organic matrix.

## 2.3 INCORPORATION OF LAYERED SILICATES INTO A POLYMER

A great amount of difficulty is associated with the complete dispersion of a layered silicate into a polymer matrix. The layered silicate, due to the presence of inorganic cations in the intralayer galleries, is hydrophilic, while the organic polymer matrix is hydrophobic. This inherent incompatibility makes it difficult to overcome the layered silicates' desired face to face stacking [8,11]. To overcome this, the inorganic cations are exchanged with alkyl onium surfactants. The alkyl onium surfactants are made up of an inorganic cation attached to an organic molecule. The inorganic cation provides a molecule capable of attaching to the silicate surface, while the alkyl group gives the gallery organic character. The alkyl onium exchanged layered silicate is referred to as an organoclay, or organically-modified layered silicate (OLS) [21]. An OLS is depicted in Figure 2.4.

The gallery region spacing, or d-spacing, of the OLS will be larger than that of the pristine layered silicate. This increase in size is controlled by two factors, the charge density of the silicate surface and the surfactant chain length [10]. A larger cation exchange capacity will allow more surfactants to reside in the clay galleries. The number of conformations available to the surfactants is decreased if there are more surfactants attached to the silicate surface. Also, a longer surfactant will cause a greater separation of silicate layers. Depending on the combination of the aforementioned factors, four orientations are possible: monolayer, bilayer, pseudo-trilayer, and a paraffin structure [7].

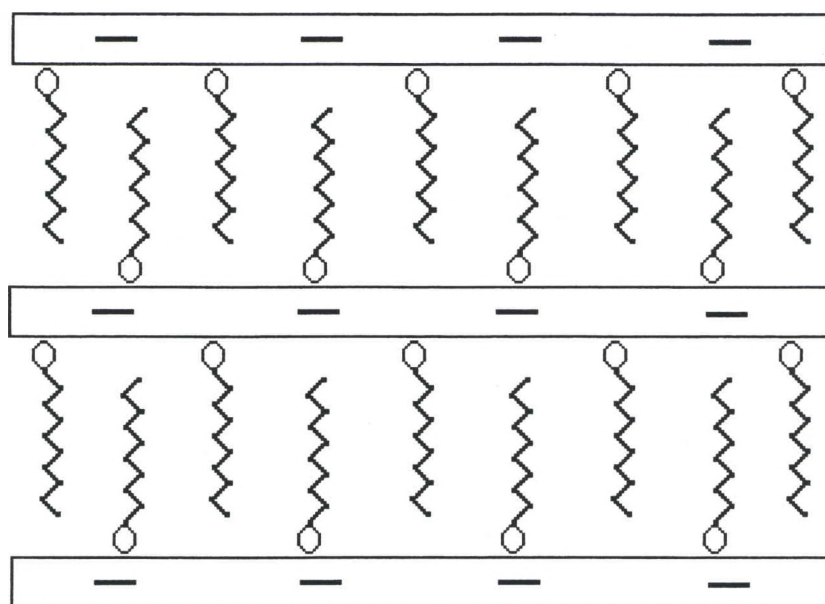


Figure 2.4. Organically-modified layered silicate

The OLS, when mixed with a compatible polymer, will intercalate the polymer [11]. Thermodynamic factors control the degree of intercalation [21]. The diffusion of a long chained monomer into a confined slit is associated with a decrease in entropy. Competing with this is an entropy increase due to the new conformational freedom of the surfactant chains. The overall entropy change will increase as the d-spacing increases. There is also an enthalpic contribution to the intercalation process. The enthalpic contribution arises from the interaction of the intercalated polymer with the surface of the layered silicate. If the polarities of the monomer and silicate surface are effectively matched, the enthalpic contribution will be negative. Combining the entropic and enthalpic contributions, the Helmholtz free energy ( $\Delta F = \Delta E - T\Delta S$ ) can be found. A decrease in the overall free energy results in a favorable process [21]. Three morphologies

are possible depending on the thermodynamics of the system investigated: immiscible, intercalated, and exfoliated or delaminated. An immiscible system results when the overall change in the free energy is positive and no monomer diffuses into the OLS galleries. An intercalated system arises when the overall change in the free energy is initially negative and subsequently increases at an intermediate d-spacing. For this system, the monomer diffuses into the intralayer galleries causing the OLS to swell until a thermodynamically stable d-spacing is achieved at which point no more monomer diffuses in. Finally, an exfoliated system is achieved when a sufficient amount of monomer diffuses into the intralayer galleries such that the d-spacing is large enough such that no van der Waals forces exist between silicate layers. In this case, the organoclay nanosheets are continuously homogeneously dispersed in the polymer matrix.

## 2.4 PREPARATION OF NANOCOMPOSITES

Three primary methods have been used to synthesize nanocomposites: exfoliation-adsorption [8,15], *in situ* intercalative polymerization [13,16], and melt intercalation [3,5].

Exfoliation-adsorption utilizes a solvent to synthesize a nanocomposite. A suitable solvent is one in which both the layered silicate and the polymer are soluble or swellable. The layered silicate is exfoliated in an excess of solvent. The monomer is then added and the solvent is subsequently evaporated. The silicate layers are prevented from reforming face to face tactoids due to the presence of the monomer. Some typical solvents include water and acetone.



*In situ* intercalative polymerization has emerged as an effective method for preparing various nanocomposite systems, including the epoxy system used in this research. For the preparation of epoxy nanocomposites, an organoclay is mixed with the polymer or a polymer/curing agent mixture at an elevated temperature, typically 60 °C-80 °C. The OLS intercalates the monomer/curing agent into the gallery region. The acidic onium ion in the intragallery region of the OLS acts as a catalyst to the polymerization reaction [10]. Thus, the intragallery polymerization occurs at an accelerated rate compared with the polymerization in the bulk polymer. If the intragallery polymerization rate is large enough, the silicate layers will be forced apart. Differential scanning calorimetry (DSC) indicates that the polymerization temperature increases with decreasing acidity of the alkylammonium cation in the order quaternary > tertiary > secondary > primary onium ions [10].

The third method by which nanocomposites have been formed is melt intercalation. A polymer in its molten state is mixed with the OLS. If the polymer and the OLS are thermodynamically compatible, an intercalated or exfoliated structure may be formed. The method is similar to *in situ* intercalative polymerization. The main difference is that melt intercalation relies on thermodynamic stability of the OLS and the polymer to drive the exfoliation process while *in situ* intercalative polymerization relies on the accelerated rate of intralayer polymerization.

## 2.5 PROPERTIES

The addition of layered silicates to polymer matrices has provided a variety of property enhancements including increased modulus [9,20], stiffness [20], improved heat distortion temperature [20], improved solvent uptake-barrier properties [14,19], and flame retardancy [2,14,22].

The increase in modulus and stiffness may be due to shear deformation and stress transfer to the platelet particles [9]. Also, the mechanical benefit has been found to be proportional to the degree of exfoliation. An exfoliated structure provides more silicate surface area available for stress transfer. Also worth noting is that better mechanical properties have been realized in polymers in their rubbery state [9]. This may be due to the alignment of the clay sheets while under strain [9]. The greatest benefit to matrices in their glassy state is provided during compressive strain [12].

The addition of layered silicates also provides a variety of barrier property enhancements. It has been proposed that the clay platelets cause a tortuous pathway for any species diffusing into the polymer [23]. This decrease in diffusion rate may result in less swelling and decreased oxidation. The clay also helps to reinforce the char formed during ablation, resulting in at least an order-of-magnitude decrease in the erosion rate of the nanocomposite when compared with the pristine polymer [22].

## 2.6 CARBON FIBER COMPOSITES

A composite is a combination of two or more materials, differing in form or composition on a macroscale [17]. The constituents retain their identities and exhibit an interface between one another. The two phases of the composites used in this research are IM7G-12k tow carbon fiber supplied by Hexcel, which is the reinforcement phase, and Epon Resin 862 / Epicure Curing Agent W, which acts as a binding matrix. The binding matrix transfers the load to and between the various fibers while protecting it from the environment [17]. The composite used can be further classified as a continuous carbon fiber composite as the length of the fibers used are equivalent to the overall dimensions of the composite.

Fiber composites offer numerous property enhancements compared with conventional materials [17]. Whereas most high strength/high stiffness materials fail due to flaw propagation, a fiber composite will not. If a single fiber fails, there are numerous bundles of fibers to carry the load. Also, fiber composites are extremely lightweight and thus have a high strength to weight ratio. Fiber composites can also be tailored to specific uses, by orientating the fibers to handle the high load directions.

## CHAPTER 3

### EXPERIMENTAL

#### 3.1 SOLVENT UPTAKE – BARRIER PROPERTIES

The effect of the addition of clay on the solvent uptake properties of Epon Resin 862 / Epicure Curing Agent W was examined. Four Epon Resin 862 / Epicure Curing Agent W panels loaded with zero percent, one percent, three percent, and six percent loadings of I.30E were provided by Dr. Chenggang Chen. From these panels, 0.5" x 1" x 0.125" coupons were cut, labeled and thoroughly dried in a vacuum oven at 100 °C. The coupons were then weighed and three coupons from each sample were placed in one of three solvents at room temperature: water, methanol, or acetone. At various times, the coupons were removed from the solvent containers, dried, weighed and replaced into the solvent containers. The degree of solvent uptake was evident due to the increased mass of the coupons over time.

#### 3.2 THERMAL OXIDATIVE STABILITY TEST

A thermal oxidative stability test was performed on three samples of Epon Resin 862 / Epicure Curing Agent W loaded with zero percent I.30E, two percent I.30E, and four percent I.30E. Five specimens of each sample, with dimensions of 1.0" x 0.5" x 0.25", were initially dried and weighed. They were then placed in

a convection oven at 200 °C and subsequently weighed at various times. From the mass-time data, the mass fluxes were calculated as a means of determining the degree of oxidation.

### 3.3 CONTINUOUS UNIDIRECTIONAL CARBON FIBER COMPOSITE PROCESSING

IM7G-12k tow / I.30E / Epon Resin 862 / Epicure Curing Agent W

unidirectional composites were processed via resin film infusion (RFI) and wet-winding. The RFI approach consisted of winding sixteen plies of IM7 fiber onto a 10" x 10" Teflon™-covered metal plate. Using silicone, a 10" x 10" dam approximately two inches in height was prepared in the autoclave. Twenty-five percent excess matrix resin was placed inside the dam and covered with nonporous Teflon™. A slit was cut into the nonporous Teflon™ to allow resin transport and the fiber plate was placed over it. The entire dam was covered with nylon to make an airtight seal. Vacuum was pulled to promote resin infiltration into the fiber bed. Pictures of the RFI layup procedure are shown in Figures 3.1, and 3.2.

The second process, wet-winding, involved feeding IM7 carbon fiber through a bath of heated Epon Resin 862 containing Epicure Curing Agent W prior to winding the fiber onto the plate. The temperature of the bath was maintained at 95 °C to optimize processability. The IM7 carbon fiber was then drawn through a glass die to control the fiber volume. As the die used was too large to achieve a fiber volume of sixty percent, only the eight central IM7 carbon

fiber plies were wound wet. After winding was complete, the fiber plate was enclosed in a nonporous Teflon™ envelope, sealed in an airtight nylon vacuum bag, and cured in an autoclave. Figures 3.3 through 3.7 show the wet-winding apparatus used in this research.

Both the RFI and wet-winding processes utilized the same autoclave curing cycle. The composites were heated to 120 °C at a rate of three degrees Celsius per minute. After a two hour hold at 120 °C, the temperature was increased to 177 °C at a rate of three degrees Celsius per minute. The temperature was then held at 177 °C for two hours and allowed to cool back to room temperature. Concurrently, the autoclave pressure was increased to 100 psi at two psi per minute and held for the duration of the curing cycle.

### 3.4 ACID DIGESTION

Acid digestion was performed to determine the volume fraction of fiber for all Epon Resin 862 / Epicure Curing Agent W / I.30E / IM7 composites and followed procedures outlined in ASTM standard D3171. Initially, all samples, approximately 1.5" x 0.5" x 0.10", were dried in a vacuum oven at 100 °C overnight and subsequently weighed. Next, they were placed in the digestion flasks with approximately 150 ml of sulfuric acid. The temperature settings were set to produce a very gentle boil and the samples were digested for approximately five hours. After allowing the acid to cool, the acid was discarded in an acid waste bottle and the remaining fiber was washed with deionized water, dried overnight in a vacuum oven at 100 °C and subsequently weighed.

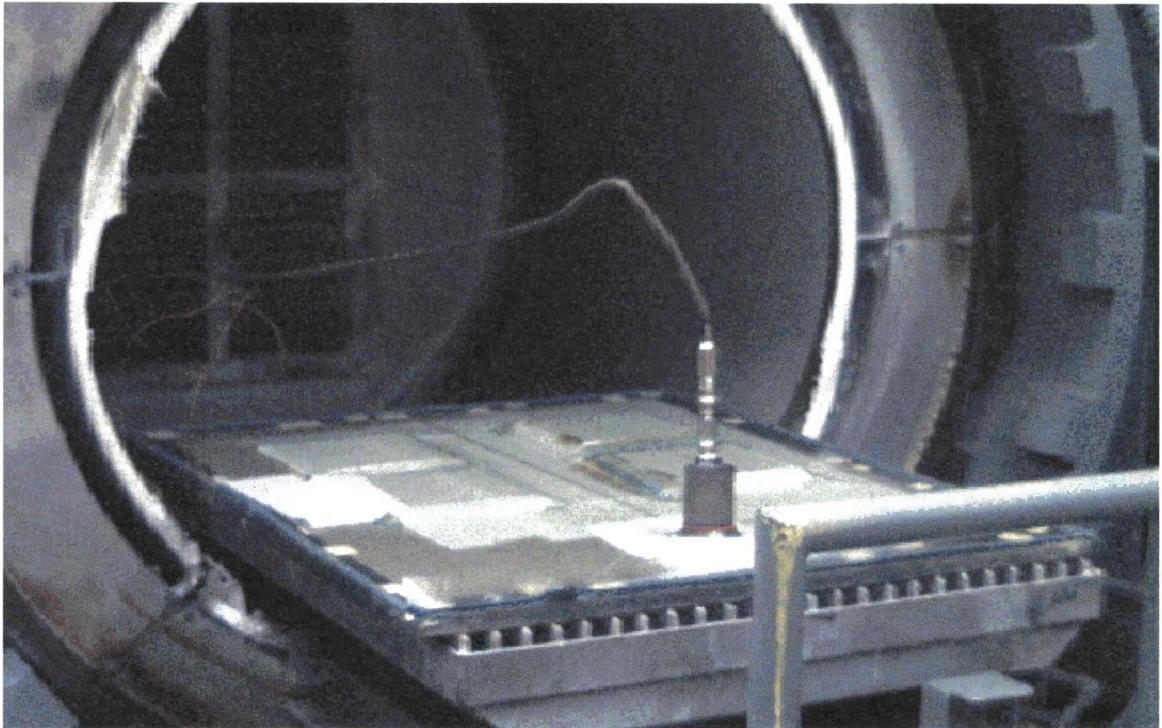


Figure 3.1. Layup procedure for RFI of epoxy-carbon fiber composite (autoclave)



Figure 3.2. Layup procedure for RFI of epoxy-carbon fiber composite





Figure 3.3 Fiber composite wet-winding apparatus

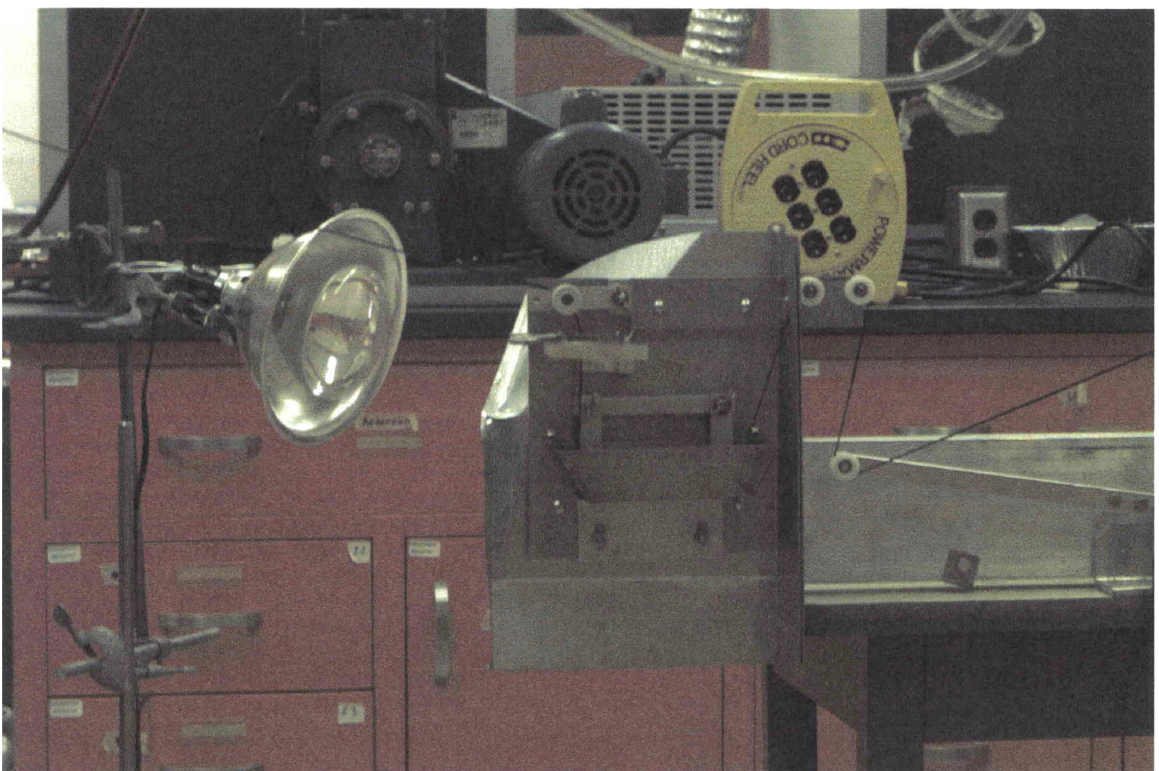


Figure 3.4. Fiber composite wet-winding apparatus (resin bath/heat lamp shown)



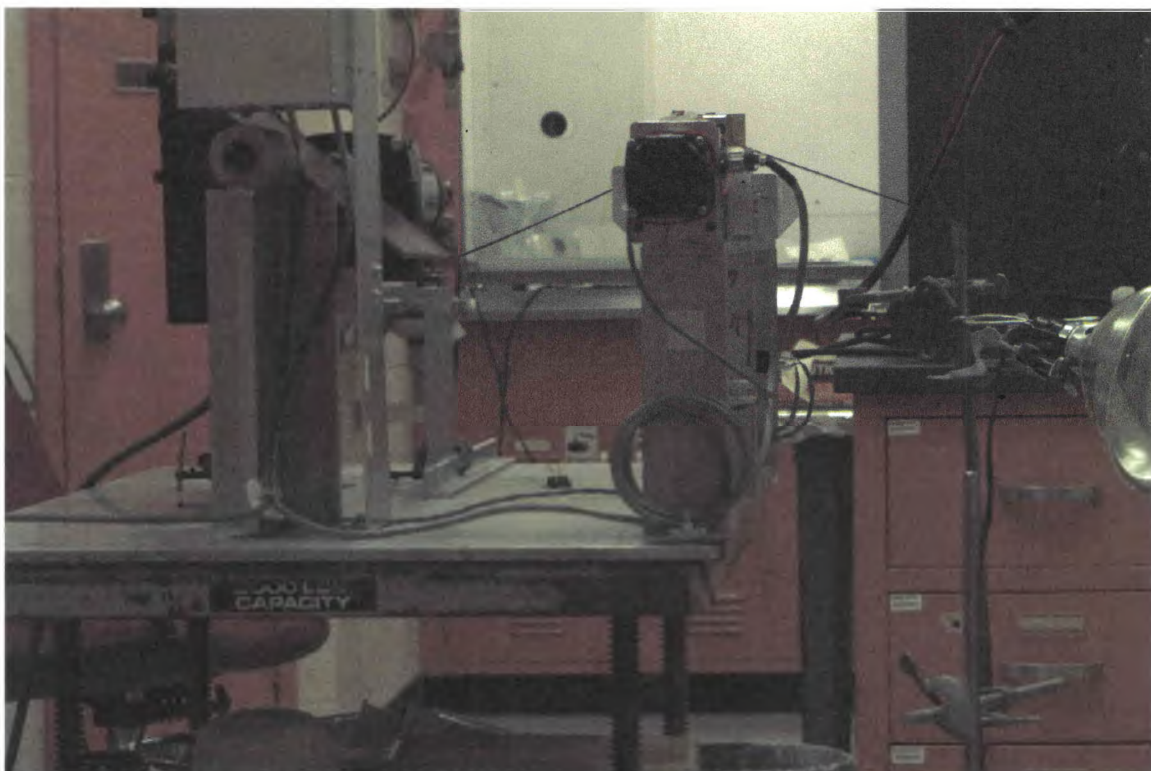


Figure 3.5. Fiber composite wet-winding apparatus (winding table)

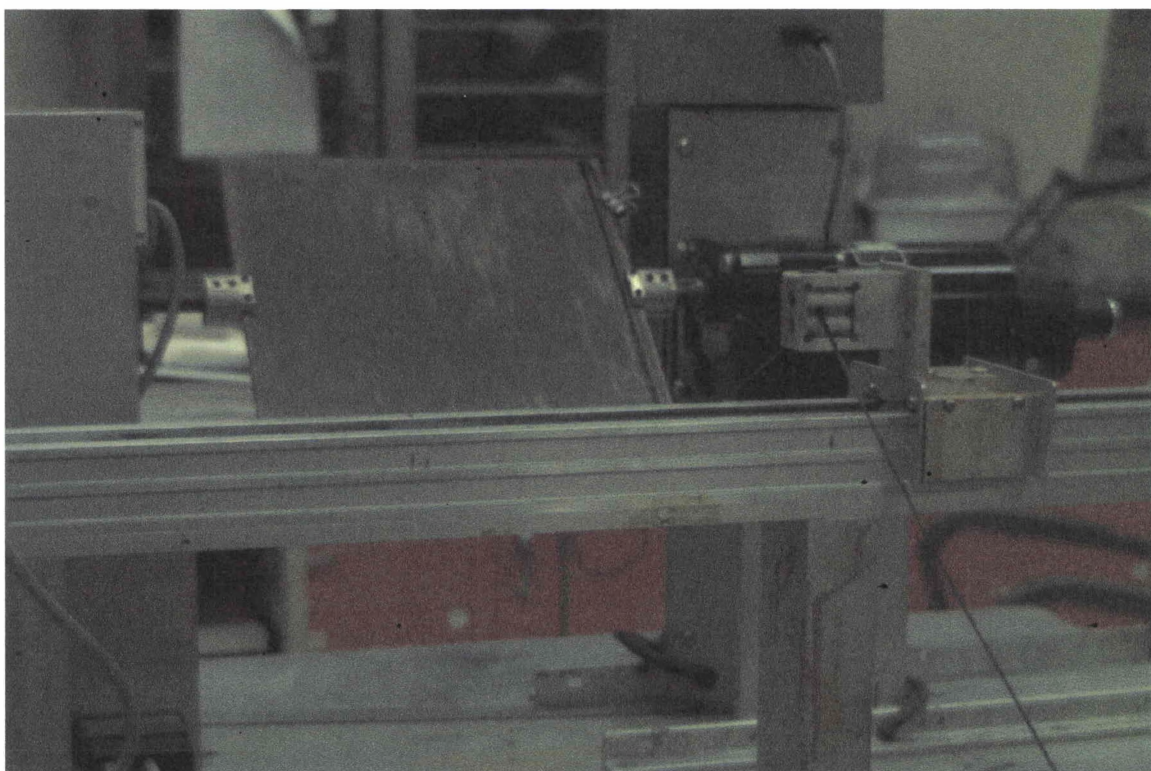


Figure 3.6. Fiber composite wet-winding apparatus (fiber plate shown)

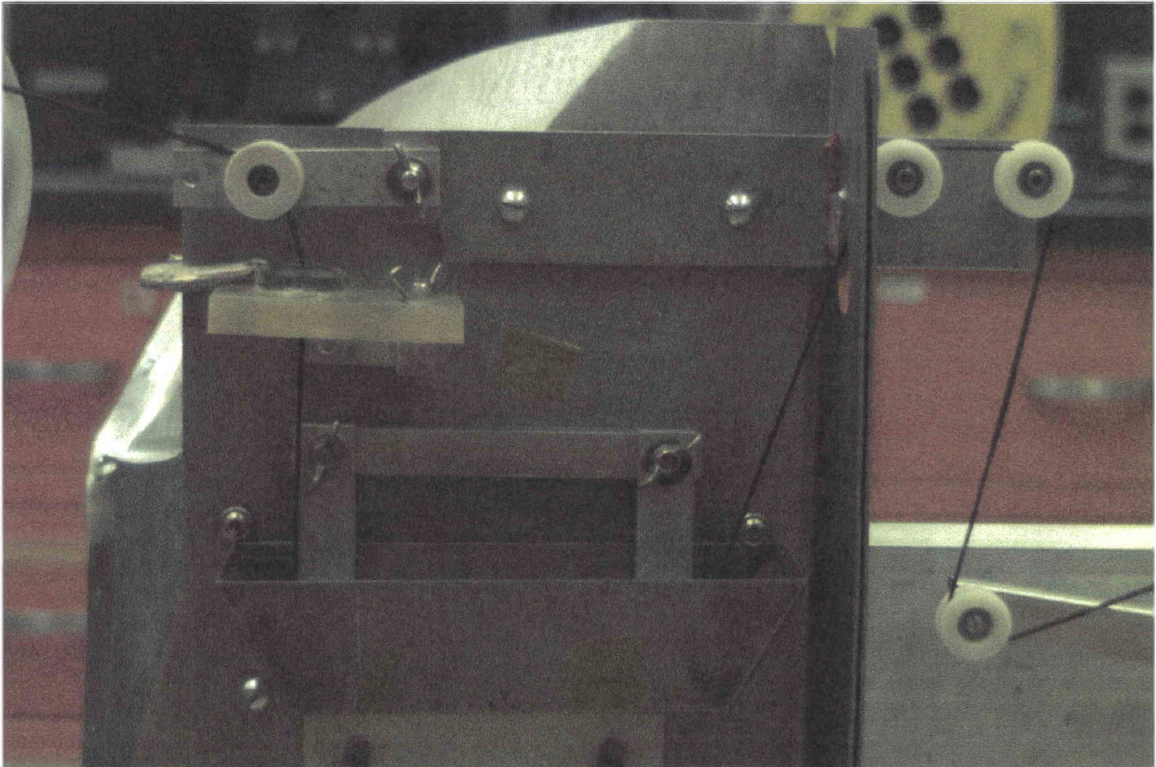


Figure 3.7. Fiber composite wet-winding apparatus(resin bath/glass die shown)

### 3.5 SCANNING ELECTRON MICROSCOPY

To examine the composite fracture surfaces, a Philips XL 30 ESEM scanning electron microscope (SEM) in Hi-vac mode at a voltage of 20 kilovolts was used. Samples were taken from the specimens which had undergone mechanical testing. The specimens were cleaned in a sonication bath and dried overnight in a vacuum oven at 100 °C before SEM micrographs were taken.

During the RFI composite processing, a concern arose that silicate filtering may have been possible as the resin infiltrated the fiber bed. A sample was collected from the carbon fiber composite which was loaded with three percent I.30E and which had been processed via RFI. Several specimens were cut from this sample, each exposing a different z-plane of the fiber composite. The EDAX



Phoenix Energy Dispersive Spectroscopy (EDS) system mounted to the SEM was used to perform an elemental analysis on the various specimens. It determined the surface concentration of selected elements, specifically silicon, oxygen, and carbon.

### 3.6 PHOTOMICROSCOPY

To further determine the quality of the carbon fiber composites, photomicrographs were collected digitally using image processing software and a Nikon Microphot-FXL optical microscope. Specimens, approximately 0.5" x 0.5", from each of the carbon fiber composite samples were potted in a fast-curing thermoset epoxy resin plug. The specimens were then sanded and polished before the photomicrographs were taken.

### 3.7 MECHANICAL TESTING

Both transverse four point flexure testing and axial four point shear testing were performed on all carbon fiber composite samples using an Instron load frame with a crosshead travel of 0.13 centimeters per minute. The tests followed ASTM standard D790. All tests consisted of ten specimens from each sample. To induce flexural failure and shear failure, a 32:1 and 16:1 span to depth ratio, respectively, was needed. Thus, the transverse flexure test specimens had dimensions of 4.5" x 0.5" x 0.10", while the axial shear test specimens had dimensions of 2.5" x 0.5" x 0.10". Once the specimens were prepared, they were

dried in a vacuum oven at 100 °C overnight before testing. All tests were done at ambient conditions.

### 3.8 THERMAL MECHANICAL ANALYSIS

Thermal analysis was performed using a TA Instruments TMA 2940 Thermomechanical Analyzer at five degrees Celsius per minute in a Nitrogen atmosphere. It was used to determine the coefficients of thermal expansion and glass transition temperatures of all fiber composites and of three Epon Resin 862 / Epicure Curing Agent W plaques loaded with zero percent I.30E, two percent I.30E, and four percent I.30E. All specimens were cut to a size of approximately 0.25" x 0.25" x 0.10". They were also cleaned in a sonication bath and dried in a vacuum oven at 100 °C overnight before testing.

## CHAPTER 4

### RESULTS AND DISCUSSION

#### 4.1 SOLVENT UPTAKE – BARRIER PROPERTIES

From the percent mass gain-time data of the nanocomposite coupons, the one-dimensional binary diffusion coefficient were found using the following relationship [6]:

$$D = \pi \cdot \left[ \frac{2h}{4M_{\max}} \right]^2 \cdot (\Delta M / \Delta t^{0.5})^2$$

D -	One-dimensional binary diffusion coefficient
$\pi$ -	Pi
h -	Half-thickness
$M_{\max}$ -	Maximum percent mass gain
$(\Delta M / \Delta t^{0.5})$ -	Initial slope of the percent mass gain verse square root time plot

The derivation of this relationship was based on the assumption of one-dimensional diffusion, which was not completely justified in this research as all coupons had an aspect ratio of approximately four in one dimension and eight in the other. An aspect ratio of ten or greater would be more desirable to ensure the validity of the assumption. Although, the one-dimensional binary diffusion

coefficients calculated may be used for a qualitative analysis. The initial slopes of the percent mass gain versus the square root of time plots were calculated using linear regression. Values for the average one-dimensional binary diffusion coefficient are listed in Table 4.1.

Table 4.1. One-dimensional binary diffusion coefficients of various solvents in Epon Resin 862 / Epicure Curing Agent W

<b>One-Dimensional Binary Diffusion Coefficient (cm<sup>2</sup>/sec)</b>			
<b>Sample</b>	<b>Water</b>	<b>Acetone</b>	<b>Methanol</b>
862/W	5.55x10 <sup>-11</sup>	1.13x10 <sup>-10</sup>	4.25x10 <sup>-11</sup>
1% I.30E	5.65x10 <sup>-11</sup>	9.10x10 <sup>-11</sup>	3.54x10 <sup>-11</sup>
3% I.30E	5.42x10 <sup>-11</sup>	6.69x10 <sup>-11</sup>	2.79x10 <sup>-11</sup>
6% I.30E	5.33x10 <sup>-11</sup>	4.63x10 <sup>-11</sup>	2.27x10 <sup>-11</sup>

As can be seen, the addition of I.30E had a dramatic effect on the ability of various solvents to diffuse into Epon Resn 862 / Epicure Curing Agent W. One exception was found in the diffusion of water into the sample loaded with one percent I.30E. It actually showed an increase of two percent in the one-dimensional binary diffusion coefficient relative to the pristine polymer system. The exact reason for this exception is unknown. For acetone and methanol, a one percent loading of I.30E decreased the diffusion coefficient by nineteen percent and seventeen percent, respectively. For a three percent loading, the diffusion coefficient decreased by two percent, forty-one percent, and thirty-four percent for water, acetone, and methanol, respectively. For a six percent loading, the diffusion coefficient loading decreased by four percent, fifty-nine percent, and forty-seven percent, respectively. The solvent uptake data for the

samples placed in acetone, methanol, and water is plotted in Figure 4.1, 4.2, 4.3 as evidence of a typical percent mass gain versus time curve.

## 4.2 THERMAL OXIDATIVE STABILITY TEST

From the mass loss data and the measured samples' dimensions, the mass fluxes were calculated and are shown in Table 4.2. The mass flux, at all times, was lowest for the Epon 862 / Epicure Curing Agent W samples followed by the samples loaded with two percent I.30E and the samples loaded with four percent I.30E. The data seems to indicate that the addition of layered silicate into an epoxy matrix does not enhance the thermal oxidative stability. However, the increased mass flux in the epoxy samples loaded with I.30E may have been due to the decomposition of the organic surfactants. Thermal analysis on a TA Instruments Hi-Res-TGA 2950 Thermogravimetric Analyzer at ten degrees Celsius per minute in Nitrogen of I.30E was performed by Dr. Chen and is shown in Figure 4.4. It showed that I.30E experienced a significant degree of mass loss at 200°C. This mass loss was due to the decomposition of the *n*-octadecylamine surfactant on the surface of the inorganic silicate. In fact, thirty-six percent of the weight was lost before an inorganic residue remained at 800 °C. Thus, the addition of layered silicates to the epoxy composite matrix may indeed enhance the thermal oxidative stability of the fiber composites. The organoclay may continue to experience decomposition of its organic surfactants while decreasing

the degree of matrix decomposition, although longer studies are needed to substantiate this hypothesis.

Table 4.2. Effects of silicate addition on thermal oxidative stability

<b>Cumulative Mass Flux at Various Times [g/(cm<sup>2</sup> · sec)]</b>					
<b>Sample</b>	<b>After 93 hrs</b>	<b>After 189 hrs</b>	<b>After 353 hrs</b>	<b>After 689 hrs</b>	<b>After 979 hrs</b>
862/W	2.50E-09	1.89E-09	1.59E-09	1.81E-09	1.96E-09
2% I.30E	3.02E-09	2.26E-09	2.06E-09	2.29E-09	2.23E-09
4% I.30E	3.50E-09	2.65E-09	2.46E-09	2.63E-09	2.38E-09

#### 4.3 ACID DIGESTION

To help determine the quality of the fiber composites, the fiber volume fraction was determined using sulfuric acid digestion. With the initial epoxy-carbon fiber composite volume, the final carbon fiber weight after digestion, and the density of the fiber (1.8 g/cm<sup>3</sup>) known, the fiber volume fraction was easily calculated. The desired fiber volume fraction was 0.60. The fiber volume fractions are listed in Table 4.3. From the data, it is clear that all fiber composites were very close to the desired volume fraction.

Table 4.3. Fiber volume fractions of Epon Resin 862 / Epicure Curing Agent W / IM7 composites

<b>Sample</b>	<b>Process Technique</b>	<b>Volume Fraction</b>
862/W/IM-7	RFI	0.604
862/W/IM-7/6% I.30E	RFI	0.599
862/W/IM-7	Wet-winding	0.603
862/W/IM-7/3% I.30E	Wet-winding	0.606
862/W/IM-7/6% I.30E	Wet-winding	0.597
862/W/IM-7/9% I.30E	Wet-winding	0.595



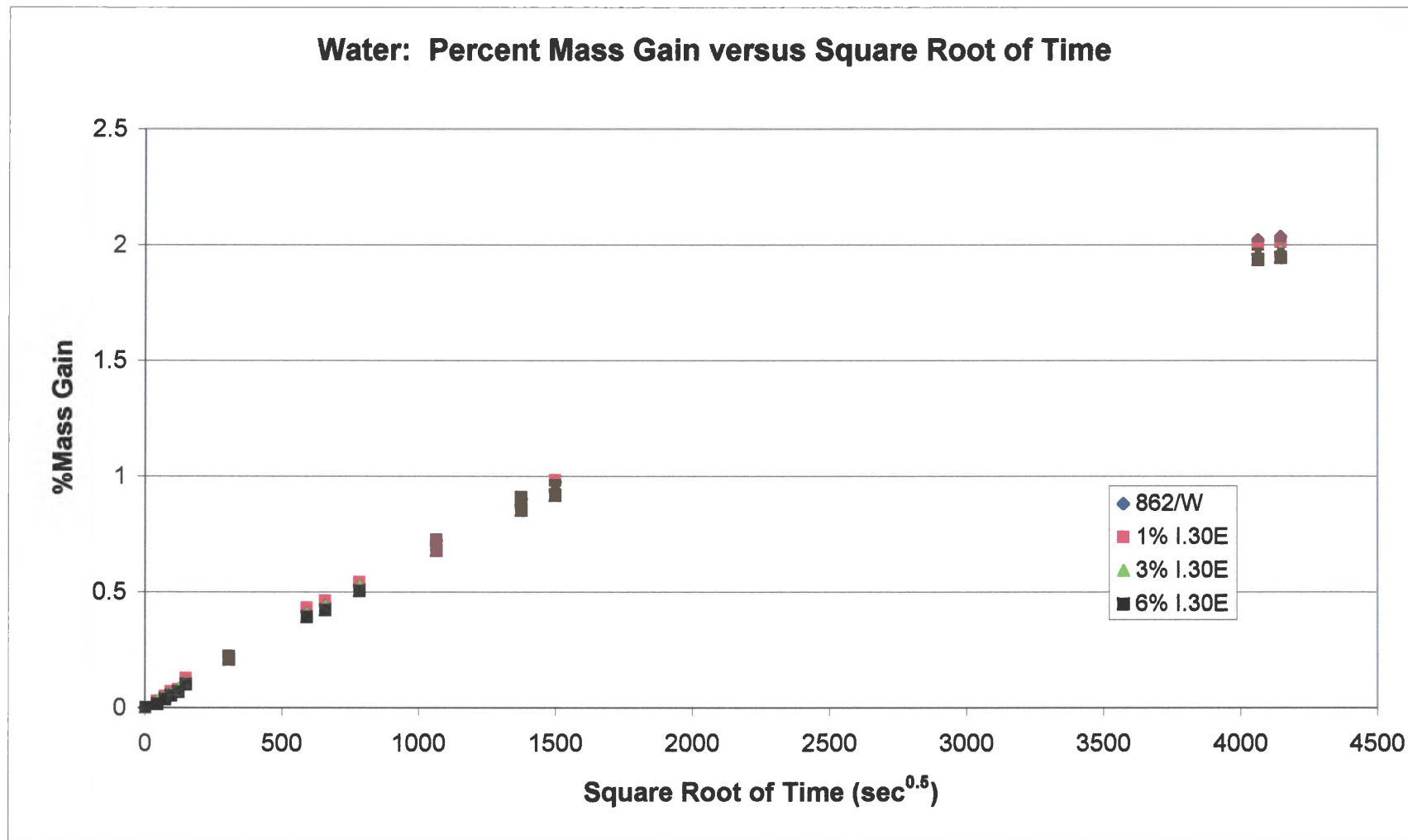


Figure 4.1. Percent mass gain versus square root of time due to diffusion of water into Epon Resin 862 / Epicure Curing Agent W loaded with 1.30E

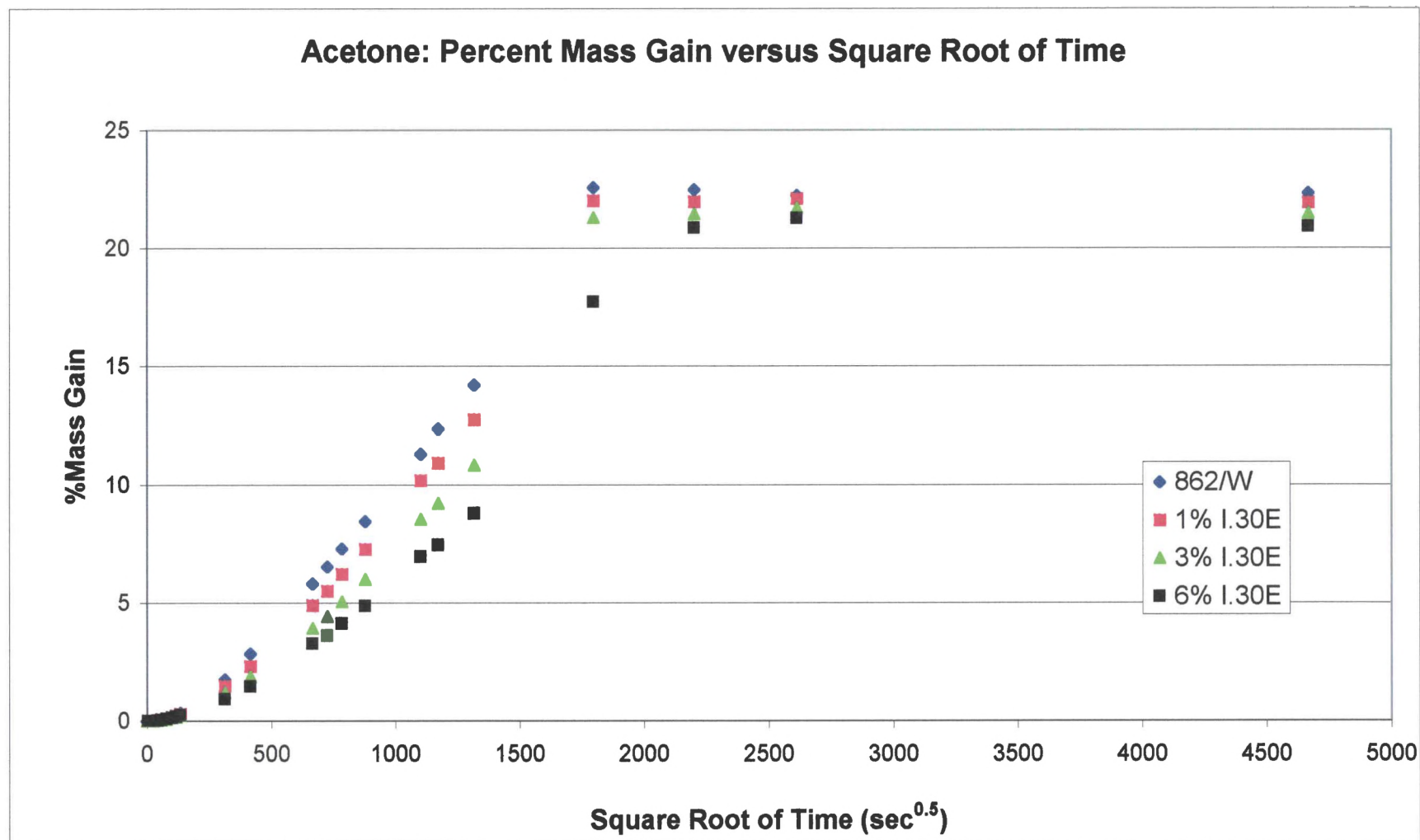


Figure 4.2. Percent mass gain versus square root of time due to diffusion of acetone into Epon Resin 862 / Epicure Curing Agent W loaded with I.30E

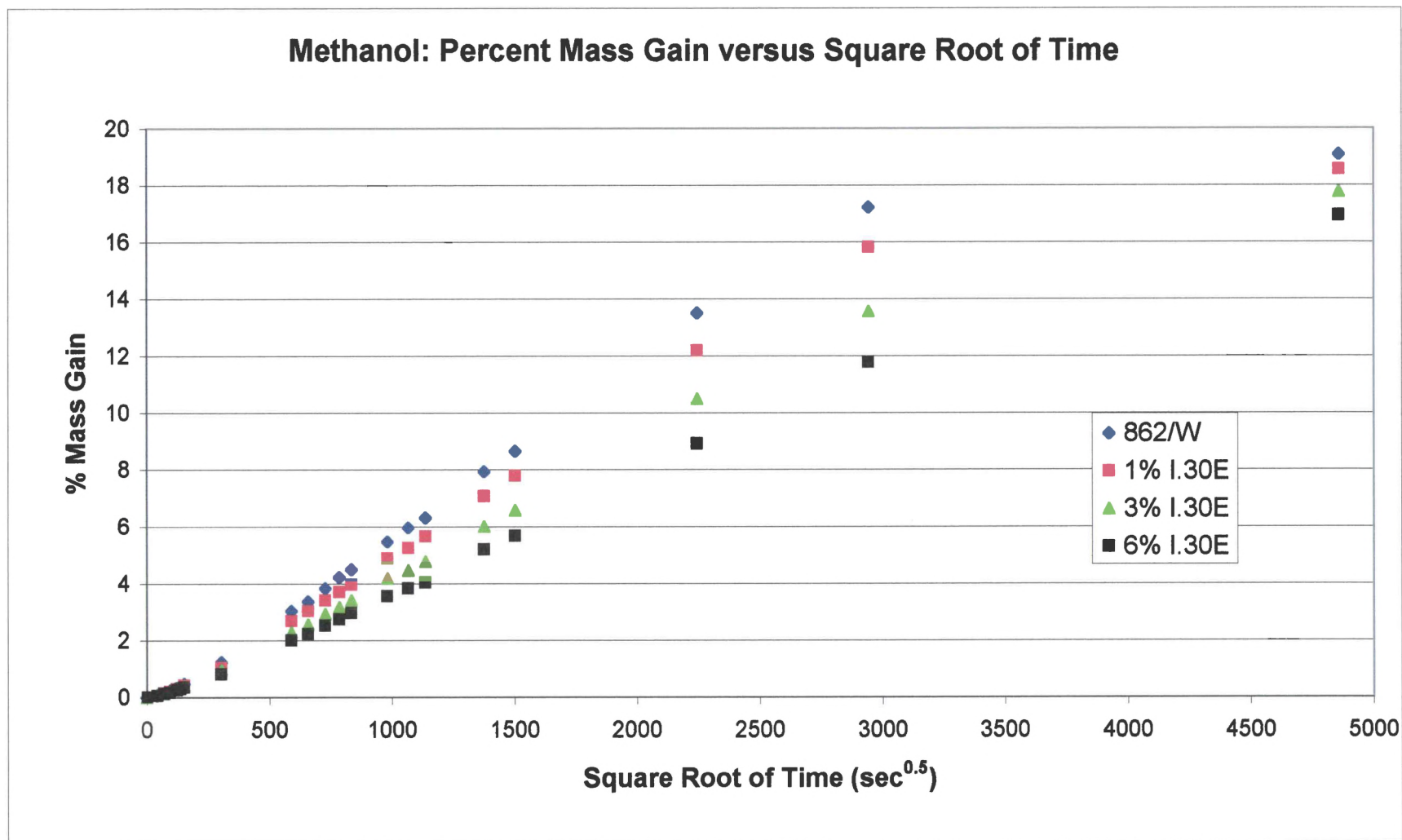


Figure 4.3. Percent mass gain versus square root of time due to diffusion of methanol into Epon Resin 862 / Epicure Curing Agent W loaded with I.30E

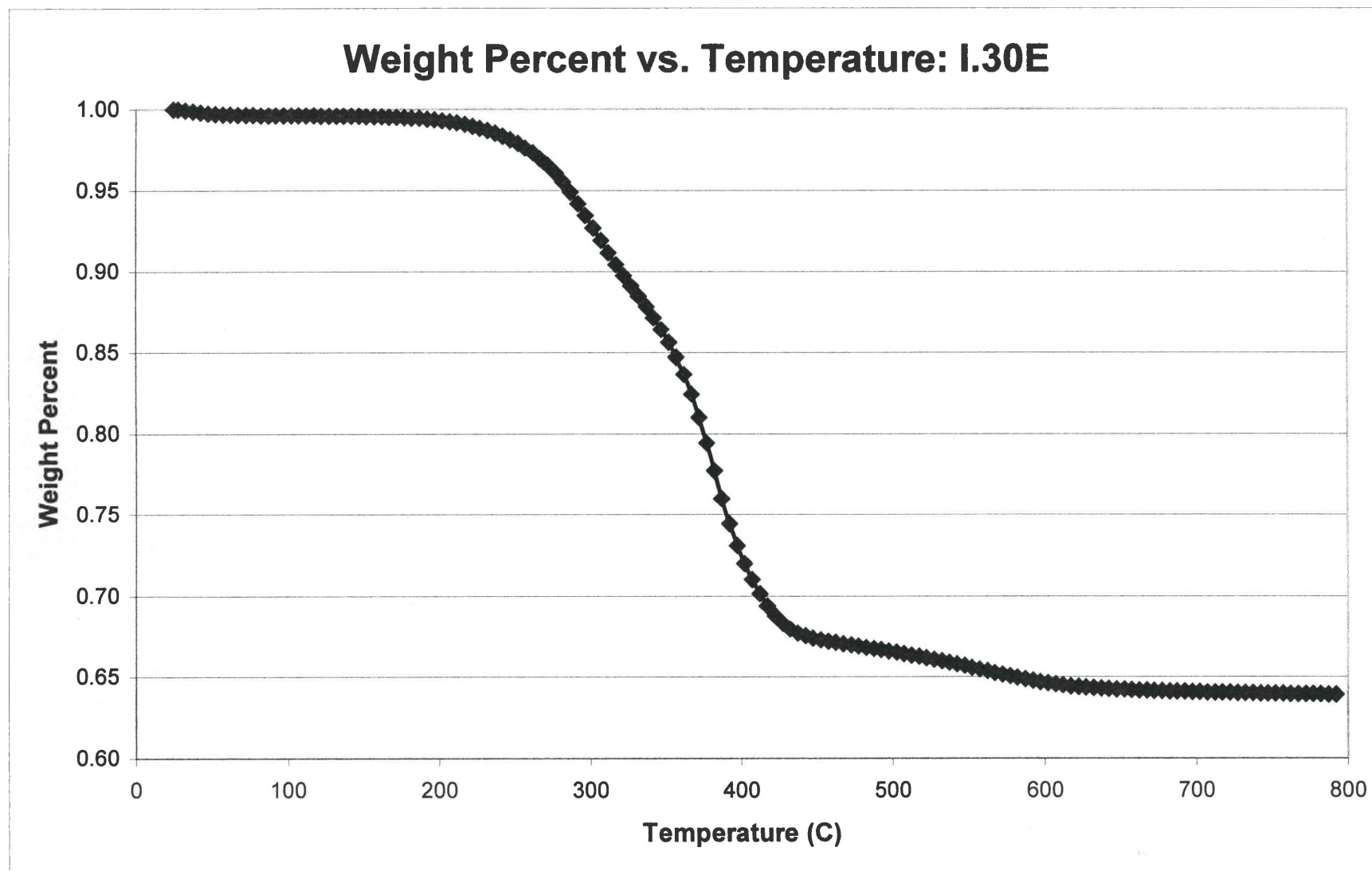


Figure 4.4. TGA results of I.30E at ten degrees Celsius per minute in a nitrogen atmosphere

#### 4.4 SCANNING ELECTRON MICROSCOPY

SEM micrographs were taken of all composite samples which had undergone mechanical testing. Under investigation was whether or not the addition of layered silicate to the Epon Resin 862 / Epicure Curing Agent W matrix altered the fracture surface characteristics of the fiber composites. Figures 4.5 through 4.10 show the SEM micrographs of shear failure surfaces of all fiber composites. After inspection, no distinct differences can be found in the fracture surfaces of the fiber composites loaded with I.30E relative to the baseline fiber composite

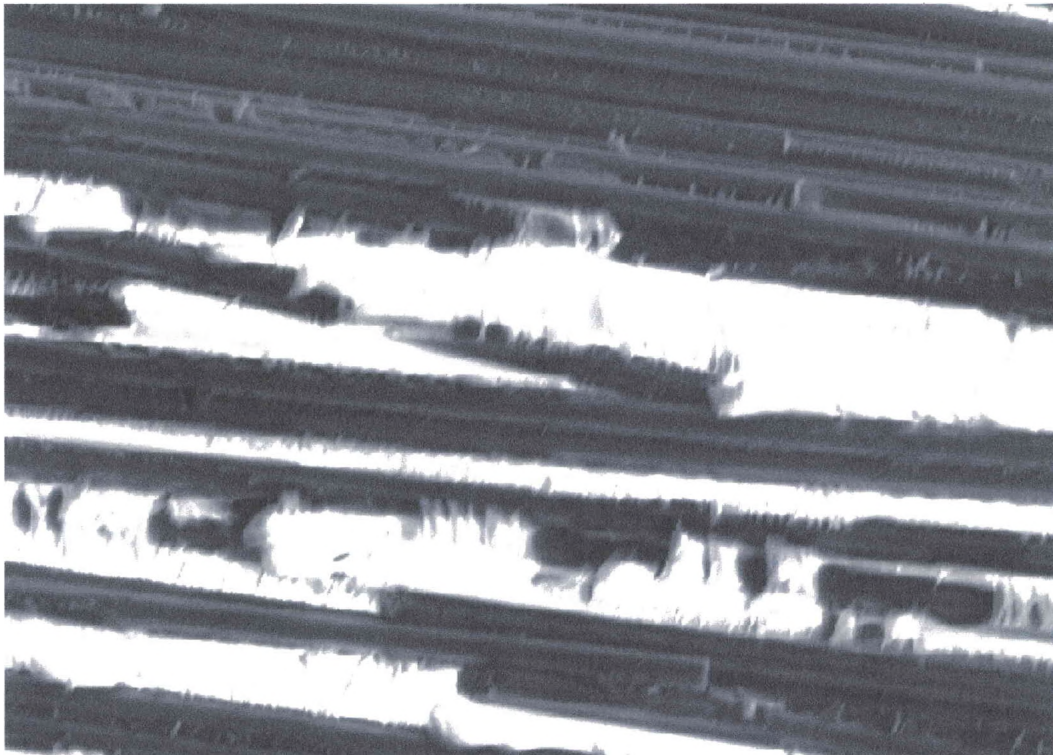


Figure 4.5. SEM micrograph of shear failure surface of Epon 862 / W / IM7 processed via resin fusion infiltration



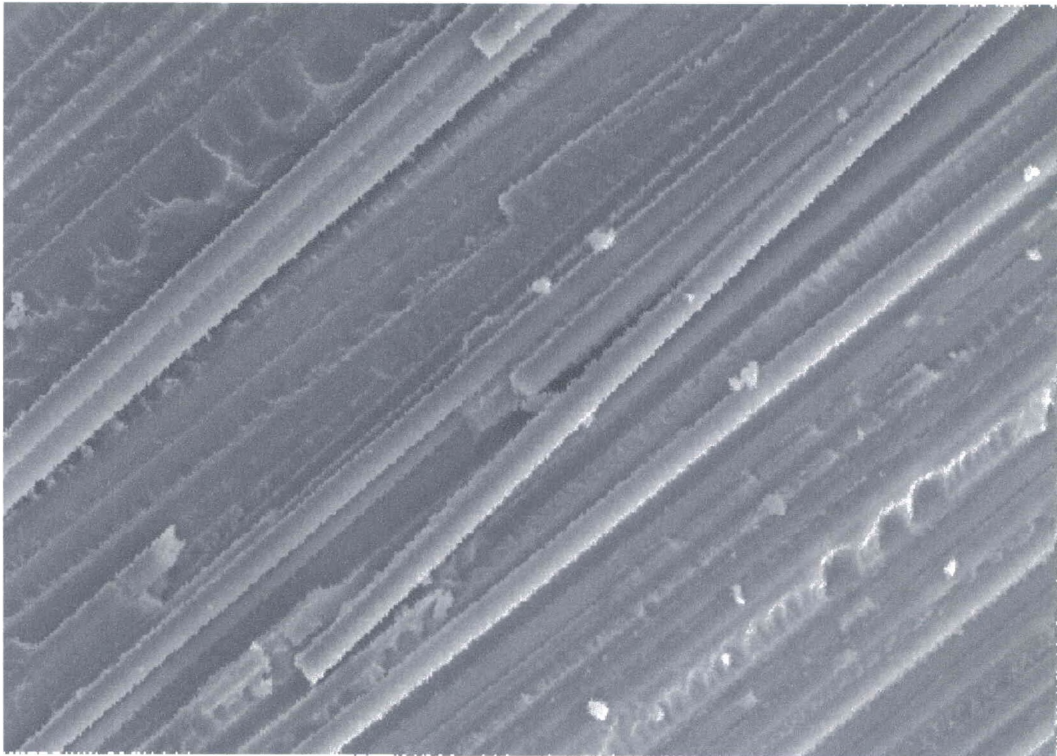


Figure 4.6. SEM micrograph of shear failure surface of Epon 862 / W / 6% I.30E / IM7 processed via resin fusion infiltration

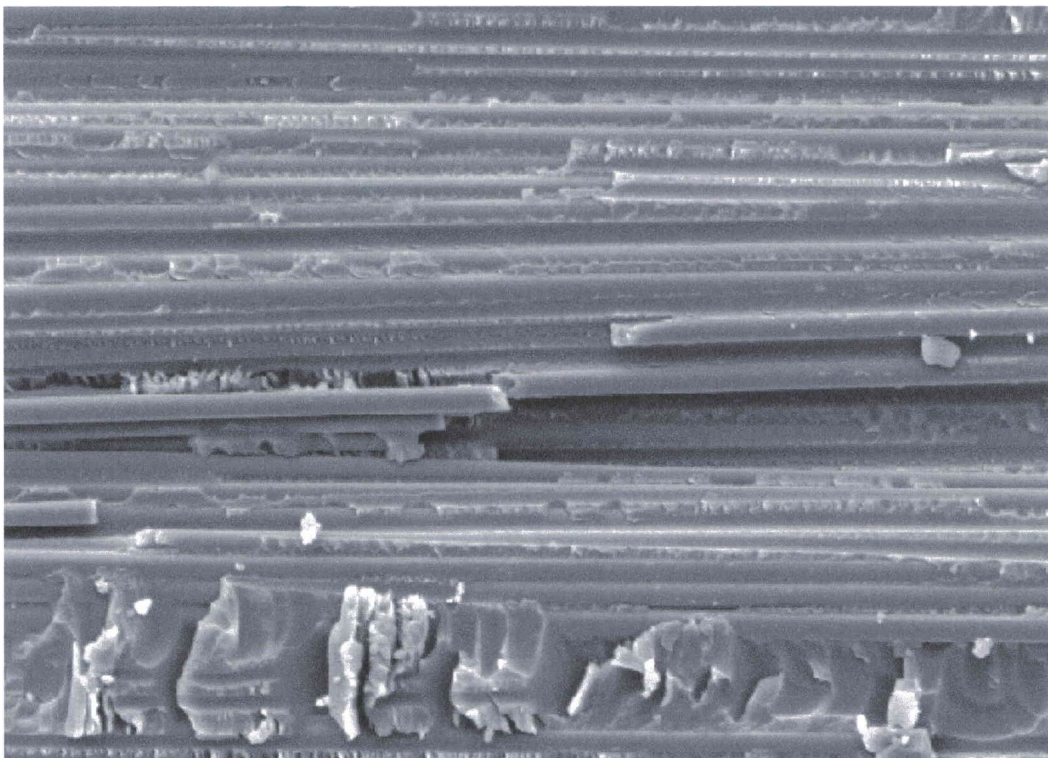


Figure 4.7. SEM micrograph of shear failure surface of Epon 862 / W / IM7 processed via wet-winding



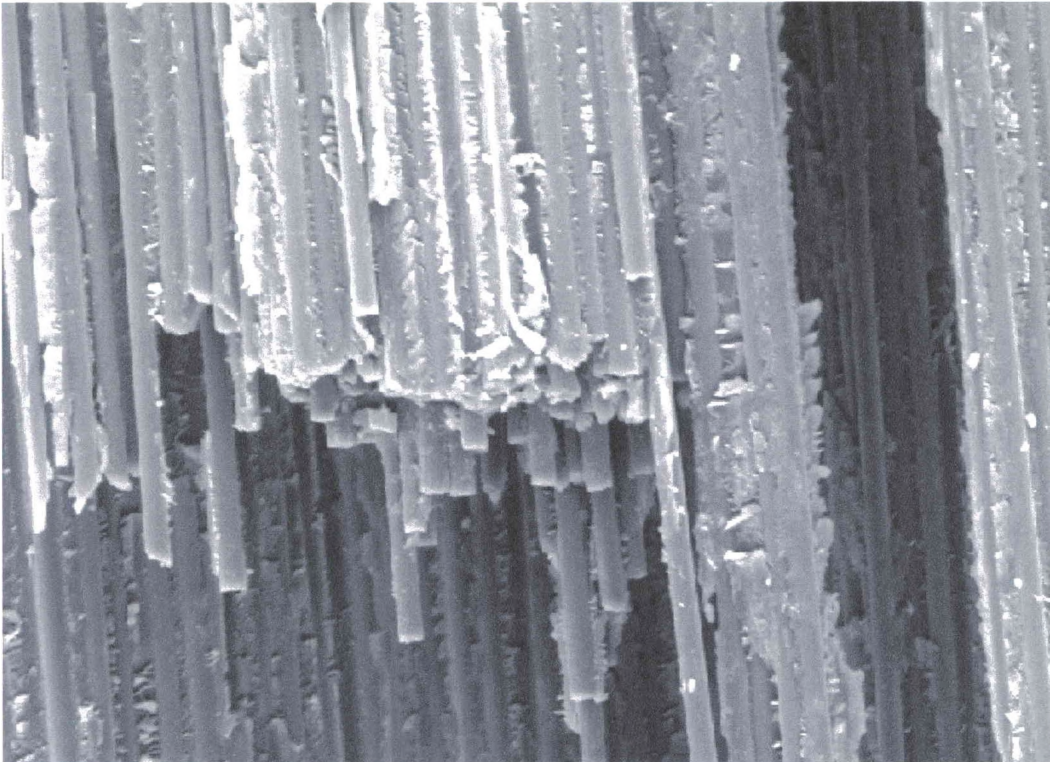


Figure 4.8. SEM micrograph of shear failure surface of Epon 862 / W / 3% I.30E / IM7 processed via wet-winding

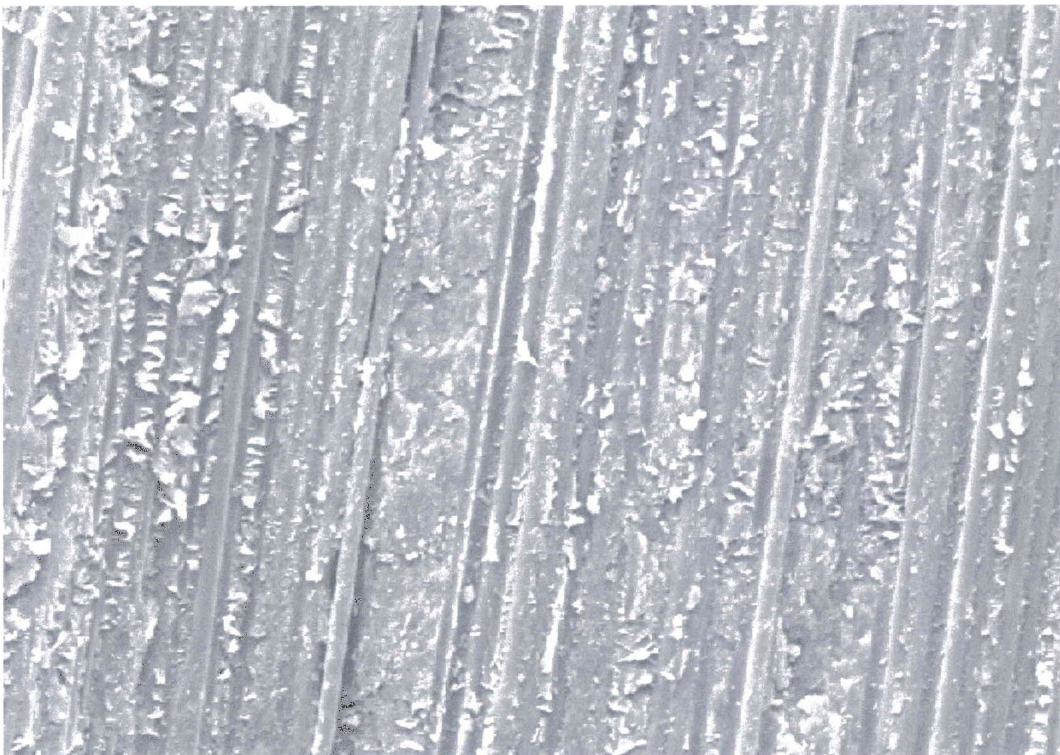


Figure 4.9. SEM micrograph of shear failure surface of Epon 862 / W / 6% I.30E / IM7 processed via wet-winding



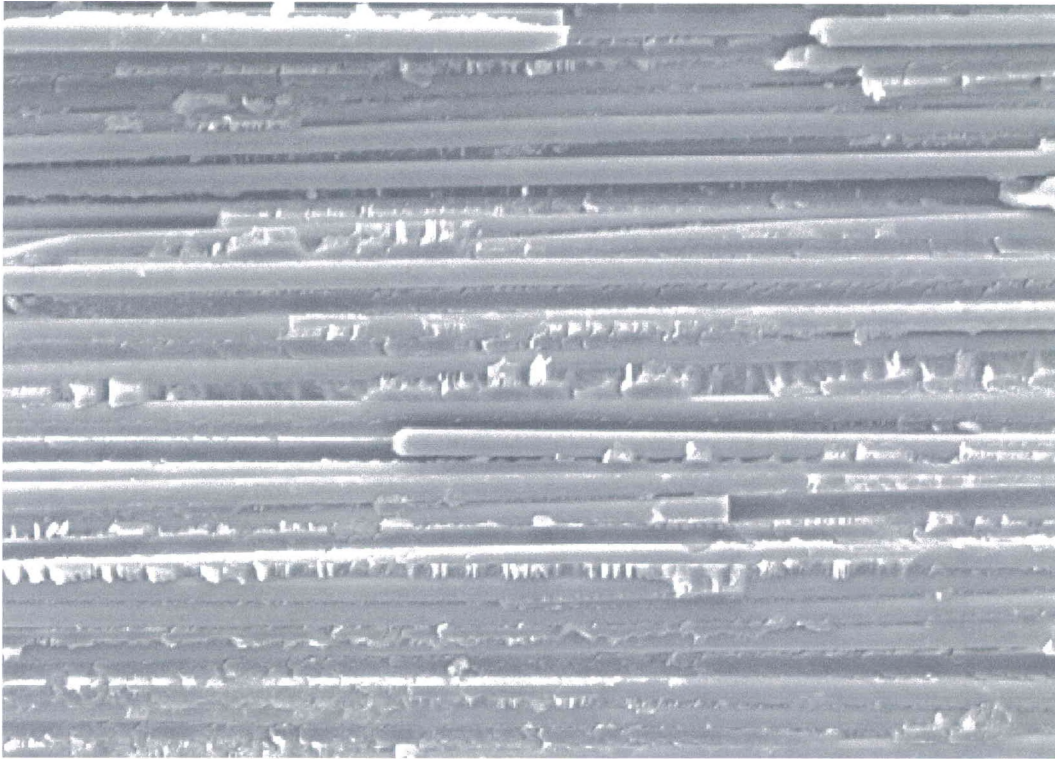


Figure 4.10. SEM micrograph of shear failure surface of Epon 862 / W / 9% I.30E / IM7 processed via wet-winding

#### 4.5 PHOTOMICROSCOPY

To further determine the quality of the Epon Resin 862 / Epicure Curing Agent W / IM7 composites, photmicrographs were taken and are shown in Figures 4.11 through 4.16. Both the composites processed via RFI appear to be of high quality. The quality of the composites processed via wet-winding, on the other hand, were not as consistent. The composites loaded with zero percent I.30E and three percent I.30E appear to be of high quality, although the composites loaded with six percent I.30E and nine percent I.30E are not of high quality. In fact, there are numerous regions throughout these composites which contain voids. One possible explanation of this decreased quality is the



increased viscosity of the Epon Resin 862 / Epicure Curing Agent W loaded with six and nine percent I.30E. The viscosity of the epoxy matrix increases by an order of magnitude with an I.30E loading of five percent. Thus, the processing may become hampered as the fiber impregnation becomes more difficult. Also, the wet-winding process can take one to two hours to wind the sixteen plies of IM7 onto the fiber plate. During this processing window, it is necessary to heat the resin in order to decrease the resin viscosity to a level where the wetted fiber will smoothly pass through the glass die. The combination of time and heat allows a degree of curing to take place, further increasing the viscosity. So, by the time the fiber plate is placed in an autoclave under pressure and allowed to completely cure out, the viscosity of the composite matrix has increased significantly. This increased viscosity may make resin flow more difficult in the composites processed via wet-winding. This problem is not encountered with the composites processed via RFI as the fiber plates and epoxy matrix are immediately placed in an autoclave for processing. Thus, the viscosity of the resin is much less for the composites processed via RFI and resin impregnation is aided.

#### 4.6 MECHANICAL TESTING

The mechanical data for the Epon Resin 862 / Epicure Curing Agent W / IM7 / I.30E unidirectional continuous fiber composites is listed in Table 4.4. The standard deviations are in parentheses. The calculations were performed using the following relationships.

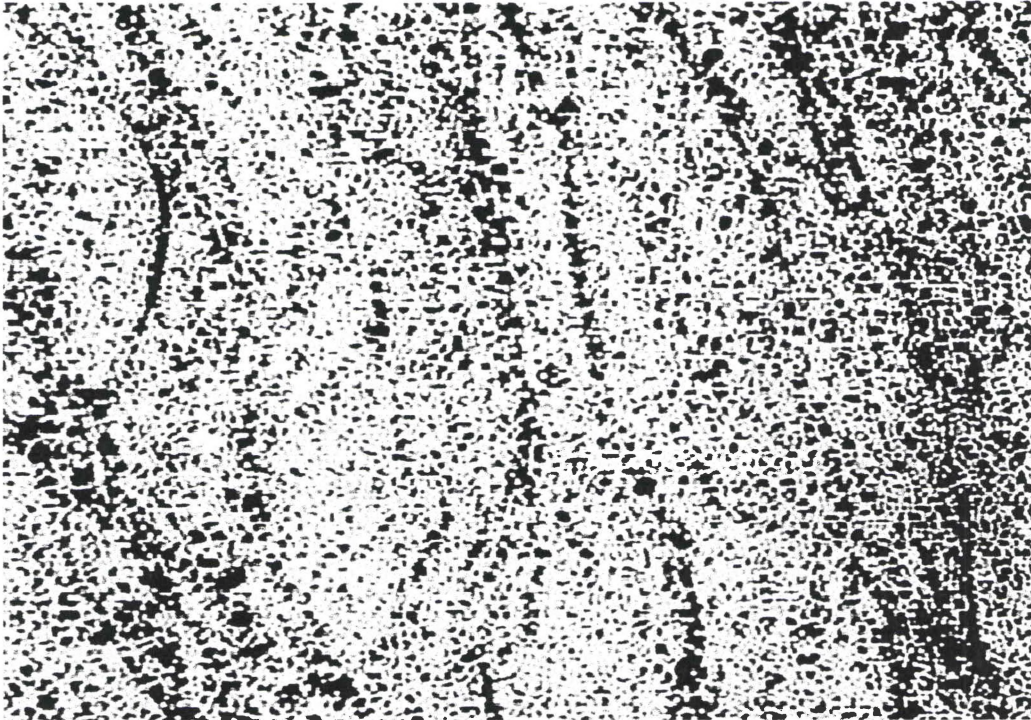


Figure 4.11. Photomicrograph of Epon 862 / W / IM7 processed via wet-winding



Figure 4.12. Photomicrograph of Epon 862 / W / 3% I.30E / IM7 processed via wet-winding



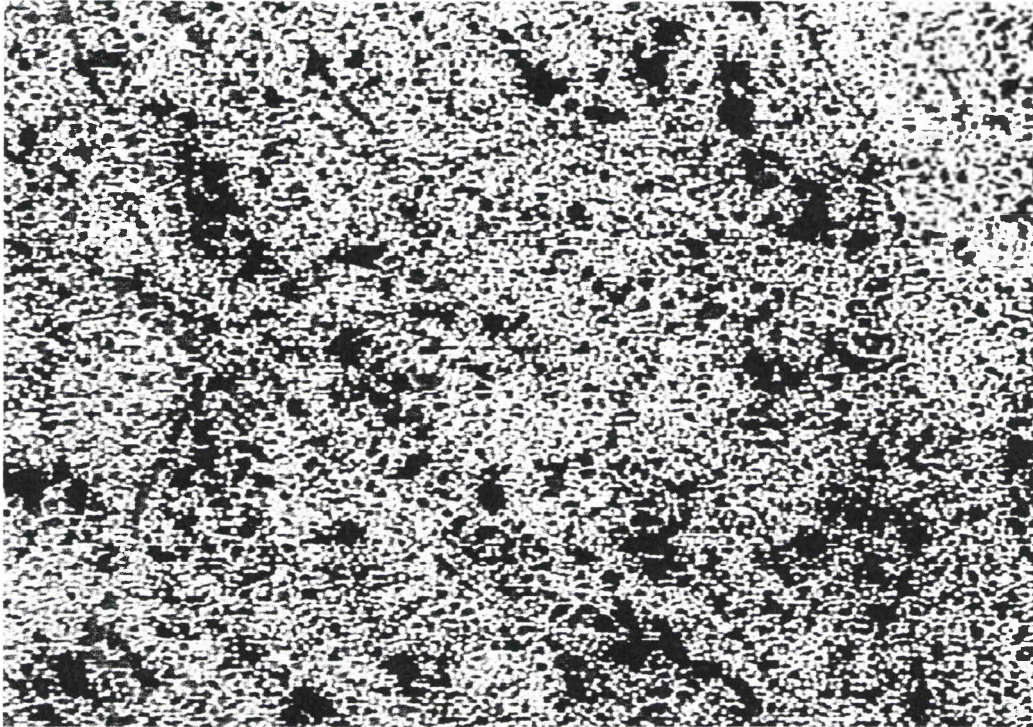


Figure 4.13. Photomicrograph of Epon 862 / W / 6% I.30E / IM7 processed via wet-winding

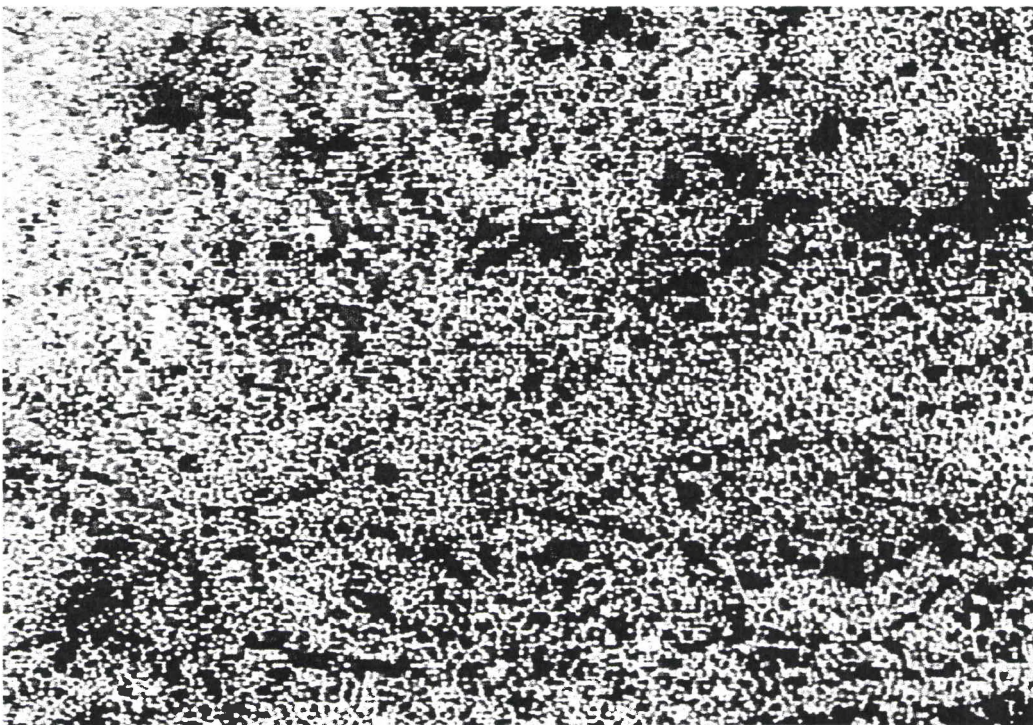


Figure 4.14. Photomicrograph of Epon 862 / W / 9% I.30E / IM7 processed via wet-winding



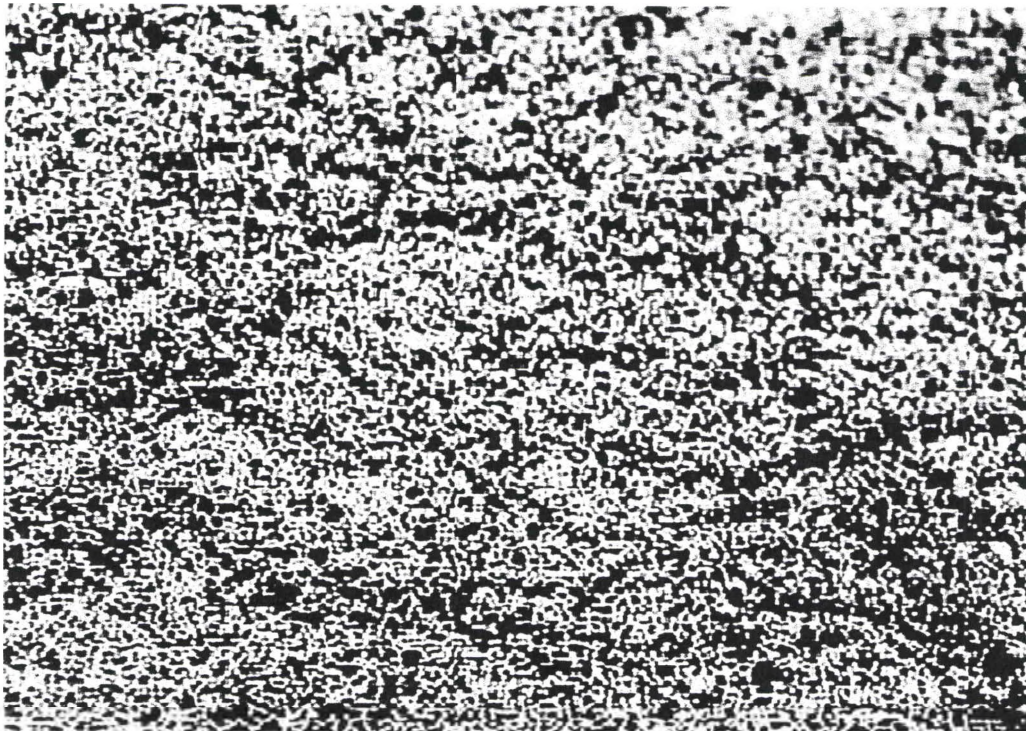


Figure 4.15. Photomicrograph of Epon 862 / W / IM7 processed via RFI

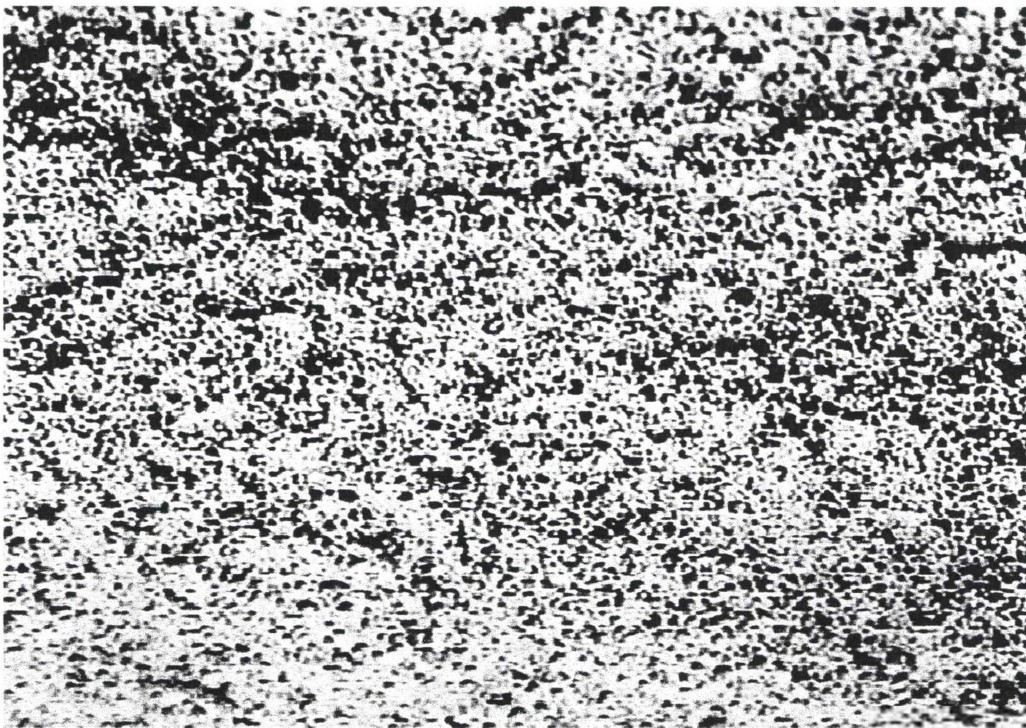


Figure 4.16. Photomicrograph of Epon 862 / W / 6% I.30E / IM7 processed via RFI

$$\text{Flex Strength} = 3PL / (4bt^2)$$

$$\text{Shear Strength} = 3P / (4bt)$$

$$\text{Modulus} = (\Delta P / \Delta v) * [L^3 / (8bt^3)]$$

The results showed an eight percent increase in the flexural strength for the six percent I.30E composites processed via RFI relative to the baseline composite, although the coefficient of variation is approximately seven percent. It also showed a five percent increase in the shear strength over the baseline composite. There was practically no difference in the modulus. The results were mixed for the composites processed via wet-winding. The fiber composites loaded with three percent I.30E, six percent I.30E, and nine percent I.30E showed a three percent decrease, two percent increase, and twenty-six percent decrease, respectively, in the flexural strength. There was a two percent increase, four percent decrease, and five percent decrease in the shear strength, respectively, relative to the baseline composite. Also, there was a two percent decrease, seven percent increase, and six percent increase in the modulus, respectively, relative to the baseline composite. The inconsistency in the data was most likely due to the poor quality of the samples processed via wet-winding. The acid digestion results showed that the composites did have a fiber volume fraction of approximately 0.60, although the photomicrographs showed that the composites, especially the composites loaded with six percent and nine percent I.30E, were poor in overall quality and homogeneity. Each had numerous regions void of any fibers.

Table 4.4. Mechanical properties of Epon 862 / W / I.30E / IM7 composites

Sample	Transverse 4PT Flex Strength (MPa)	Transverse 4PT Flex Modulus (GPa)	Axial 4PT Shear Strength (MPa)
862/W/IM-7(RFI)	84.8 (6.9)	7.31 (0.50)	66.1 (2.9)
862/W/IM-7/6% I.30E(RFI)	91.7 (5.4)	7.38 (0.43)	69.6 (2.6)
862/W/IM-7(WW)	79.3 (4.2)	7.65 (0.52)	69.0 (2.1)
862/W/IM-7/3% I.30E(WW)	77.2 (3.3)	7.52 (0.64)	70.3 (2.9)
862/W/IM-7/6% I.30E(WW)	80.7 (4.9)	8.21 (0.79)	66.2 (2.0)
862/W/IM-7/9% I.30E(WW)	58.7 (7.3)	8.14 (0.61)	65.5 (2.1)

#### 4.7 THERMAL MECHANICAL ANALYSIS

Listed in Table 4.5 are the glassy state and rubbery state coefficients of thermal expansion along with the glass transition temperatures of all fiber composite samples and three Epon Resin 862 / Epicure Curing Agent W resin plaques loaded with zero percent I.30E, two percent I.30E, and four percent I.30E.

The data for the resin plaques showed three tenths of a percent decrease and three percent decrease in the glassy state CTE for the plaques loaded with two percent I.30E and four percent I.30E, respectively, relative to the baseline system. There was a five percent decrease and four percent decrease in the rubbery state CTE for the plaques loaded with two percent I.30E and four percent I.30E, respectively, relative to the baseline system. Also, the glass transition temperature decreased by five percent and nine percent, respectively, relative to the baseline.

For the samples processed via RFI, the glassy state CTE of the Epon Resin 862 / Epicure Curing Agent W / IM7 fiber composite loaded with six



percent I.30E decreased eleven percent relative to the baseline, while the rubbery state CTE decreased twenty-two percent. The glass transition temperature of the fiber composite loaded with six percent I.30E decreased three percent relative to the fiber composite with no I.30E.

The data from the fiber composite samples processed via wet-winding showed mixed results. The glassy state CTE of the fiber composite loaded with three percent I.30E, six percent I.30E, and nine percent I.30E increased one percent, increased fourteen percent, and increased twenty percent relative glassy state CTE of the fiber composite with no I.30E loading.

From the data of the resin plaques and the fiber composites processed via RFI, it appeared as though the addition of layered silicates significantly decreased the CTE's of the composite matrix. The effect was amplified for the rubbery state CTE's. The inconsistencies found in the fiber composite samples processed via wet-winding were most likely due to the poor quality of the composites relative to the composites processed via RFI.

Table 4.5 Thermal-mechanical analysis of fiber composites and resin plaques

Sample	Sample Type	Glassy State CTE( $\mu\text{m}/\text{m}^{\circ}\text{C}$ )	Rubbery State CTE( $\mu\text{m}/\text{m}^{\circ}\text{C}$ )	Tg ( $^{\circ}\text{C}$ )
862 / W	Resin Plaque	72.1	175	151.9
862 / W / 2% I.30E	Resin Plaque	71.9	166	144.6
862 / W / 4% I.30E	Resin Plaque	70.2	168	138.0
862 / W / IM7	RFI	46.9	122	142.4
862 / W / IM7 / 6% I.30E	RFI	41.8	95.3	137.6
862 / W / IM7	Wet-winding	34.2	100	146.3
862 / W / IM7 / 3% I.30E	Wet-winding	34.5	82.8	142.9
862 / W / IM7 / 6% I.30E	Wet-winding	38.9	97.6	140.1
862 / W / IM7 / 9% I.30E	Wet-winding	41.2	110	140.2

## CHAPTER 5

### CONCLUSIONS

The incorporation of layer silicates into aerospace composite matrices offers new hope in the tailorability and enhancement of carbon fiber composites over those presently used. In this research, the characterization of a continuous unidirectional Epon Resin 862 / Epicure Curing Agent W / IM7G-12k tow / I.30E fiber composite processed via resin fusion infiltration and wet-winding was performed. Overall, the addition of I.30E to Epon Resin 862 / Epicure Curing Agent W did indeed offer improvements over the baseline system composite matrix, although it failed to significantly improve the matrix dominated mechanical properties of the carbon fiber composite. Two key areas where the addition of layer silicates offered significant improvements included decreased solvent diffusion coefficients and decreased coefficients of thermal expansion. The fiber composites loaded with I.30E and processed via resin fusion infiltration showed statistically insignificant increases in the transverse four point flex strength and axial four point shear strength. Composites processed via wet-winding produced mixed mechanical results, although photomicroscopy showed that the composite quality for these samples was poor. It is also unclear as of yet whether or not there is any benefit in the thermal oxidative stability from the addition of layer silicates as further testing is required. Future research will focus on adding



coupling agents to the organoclay to increase adhesion to the matrix. High shear mixing will also be investigated as a means of achieving a more desirable organoclay morphology.

## REFERENCES

1. Alexandre, Michael, Philippe Dubois, 2000. Polymer-Layered Silicate Nanocomposites: Preparation, Properties and Uses of a New Class of Materials. *Materials Science and Engineering*, 1-63.
2. Gilmann, J.W., T. Kashiwagi, 1997. Nanocomposites: A Revolutionary New Flame Retardant Approach. *SAMPE Journal* 33 No. 4, 40-46.
3. Hasegawa, N., M. Kawasumi, M. Kato, A. Usuki, A. Okada, 1998. Preparation and mechanical properties of polypropylene-clay hybrids using a maleic anhydride-modified polypropylene oligomer. *J. Appl. Polym. Sci.* 67, 87-92.
4. Kaviratna, P.D., Thomas J. Pinnavaia and P.A. Schroeder, 1996. Dielectric Properties of Smectite Clays. *J. Phys. Chem. Solids* 57, 1897-1906.
5. Kawasumi, M., N. Hasegawa, M. Kato, A. Usuki, A. Okada, 1997. Preparation and mechanical properties of polypropylene-clay hybrids. *Macromolecules* 30, 6333-6338.
6. Kresse, Candace Sue, 1991. Comparison of experimental, analytical, and numerical solutions for water diffusion in composite materials. University of Dayton Chemical Engineering Masters Thesis.
7. Lagaly, Gerhard, 1986. Interaction of alkyamines with different types of layered compounds. *Solid State Ionics* 22, 43-51.
8. Lagaly, Gerhard, 1999. Introduction: From Clay Mineral-Polymer Interactions To Clay Mineral-Polymer Nanocomposites. *Applied Clay Science* 15, 1-9.
9. Lan, T., T.J. Pinnavaia, 1995. Clay-reinforced epoxy nanocomposites. *Chem. Mater.* 6, 2216-2219.
10. Lan, Tie, Padmananda D. Kaviratna and Thomas J. Pinnavaia, 1996. Epoxy Self-Polymerization In Smectite Clays. *J. Phys. Chem. Solids* 57, 1005-1010.

11. Lebaron, Peter C., Zhen Wang, and Thomas J. Pinnavaia, 1999. Polymer-layered Silicate Nanocomposites: An Overview. *Applied Clay Science* 15, 11-29.
12. Massam, J., T.J. Pinnavaia, 1998. Clay nanolayer reinforcement of a glassy epoxy polymer. *Mater. Res. Soc. Symp. Proc.* 520, 223-232.
13. Messersmith PB, E.P. Giannelis, 1994. Synthesis and characterization of layered silicate-epoxy nanocomposites. *Chem Mater.* 6, 1719-1725.
14. Okada, A., A. Usuki, 1995. The chemistry of polymer-clay hybrids. *Mater. Sci. Eng., C* 3, 109-115.
15. Okata, N., S. Kawakage, T. Ogihara, 1997. Poly(vinyl alcohol)-clay and poly(ethylene oxide)-clay blend prepared using water as solvent. *J. Appl. Polym. Sci.* 66, 573-581.
16. Okamoto, Masami, Satoshi, Morita, Hideyuki Taguchi, Yong Hoon Kim, Tadao Kotaka, and Hiroshi Tateyama, 2000, Synthesis and structure of smectic clay/poly(methyl methacrylate) and clay/polystyrene nanocomposites via in situ intercalative polymerization, *Polymer* 3887-3890.
17. Reinhart, T.J., L.L. Clements, 1987. Introduction to Composites, *Engineered Materials Handbook: Composites*, Vol. 1, 27-34.
18. Shell Product Literature, SC: 772, <http://www.resins-versatics.com/resins/resins.nsf/Literature/SC%3A772?OpenDocument-SC772>
19. Usuki, A., M. Kawasumi, Y. Kojima, A. Okada, T. Kurauchi, O. Kamigaito, 1993a. Swelling behavior of montmorillonite exchanged for  $\omega$ -amino acids by  $\epsilon$ -caprolactam. *J. Mater. Res.* 8, 1174.
20. Usuki, A., Y. Kojima, M. Kawasumi, A. Okada, Y. Fukushima, T. Kurauchi, O. Kamigaito, 1993b. Synthesis of nylon 6-clay hybrid. *J. Mater. Res.* 8, 1179.
21. Vaia, R.A., E.P. Giannelis, 1997. Polymer melt intercalation in organically-modified layered silicates: Model predictions and experiment. *Macromolecules* 30, 8000-8009.
22. Vaia, R.A., G. Price, P.N. Ruth, H.T. Nguyen, J. Lichtenhan, 1999. Polymer/layered silicate nanocomposites as high performance ablative materials. *Applied Clay Science* 15, 67-92.

23. Yano, K., A. Usuki, A. Okada, T. Kurauchi, O. Kamigaito, 1993. Synthesis and properties of polyimide-clay hybrid. *J. Polym. Sci., Part A: Polym. Chem.* 31, 2493-2498.